Development and Applications of Fluorinated Oligomeric Nanocomposites Imparted by Ionic Liquids

Doctoral Course
Graduate School of Science and Technology
Hirosaki University

Doctor Thesis

March 2017

Yoshitaka Sutoh

Contents

General Introduction

1. Development of Ionic Liquids

Ionic liquids (room temperature ionic liquids) are salts in which the ions are poorly coordinated, resulting in a variety of solvents being liquid below 100 °C, or even at room temperature. Cation or anion has a delocalized charge and one component is organic, which prevents the formation of a stable crystal lattice. For example, the melting point of 1-ethyl-3-methylimidazolium chloride is 84 ^{o}C and is solid at room temperature. However, salt as the liquid by replacing chloride anion in the imidazolium chloride as bis(trifluoromethanesulfonyl)imide anion is isolated.[1, 2)]

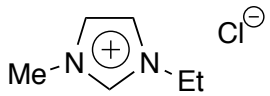

1-Ethyl-3-methylimidazolium chloride

mp: 84 ^{o}C

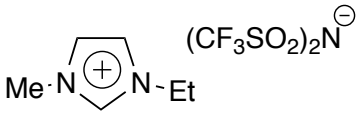

1-Ethyl-3-methylimidazolium bis(trifluoromethanesulfonyl)imide

mp: -15 ^{o}C (liquid at room temperature)

Therefore, a wide variety of ionic liquids can be easily synthesized through the combination of numerous cations and anions. In fact, as shown in Fig. 1, the imidazolium-, pyrazolium-, ammonium-, and phosphomium-types ionic liquids have been already reported,

and their unique properties and applications have been comprehensively studied, so far.[1, 2] Especially, ionic liquids are thermally stable solvents and as such as very promising replacements for the traditional volatile organic solvents.[3 ~ 9] From this point of view, ionic liquids have been used as media for the homogeneous catalytic reactions.[10, 11]

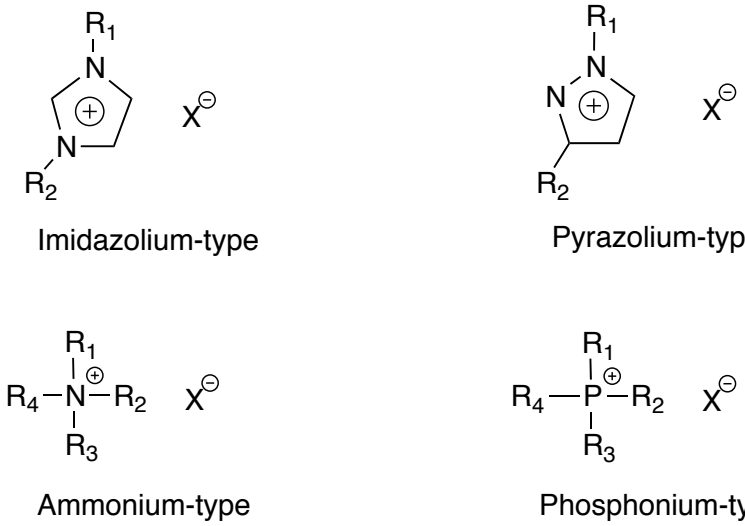

Fig. 1 Classification of traditional ionic liquids into their structures

2. Development of ionic liquid composites

Ionic liquids have been hitherto used as catalysts in organic synthetic reactions.[12, 13] The high viscosity of ionic liquids may cause mass transfer problem. Thus, the immobilization of ionic liquids onto the solid support has some advantages through the easily tunable acidity and the enhancement of hydrophilicity or hydrophobicity of the solid surface

by changing the length of side chains of the inorganic cation.[14 ~ 18] For example, 1,2-dimethyl-3-(3-triethoxysilylpropyl)imidazolium chloride, which was synthesized by the reaction of 1,2-dimethylimidazolium chloride with 3-chloropropyltriethoxysilane, was grafted onto the silica particle surface by using the sol-gel reaction with silica particles as shown in Scheme 1.[19]

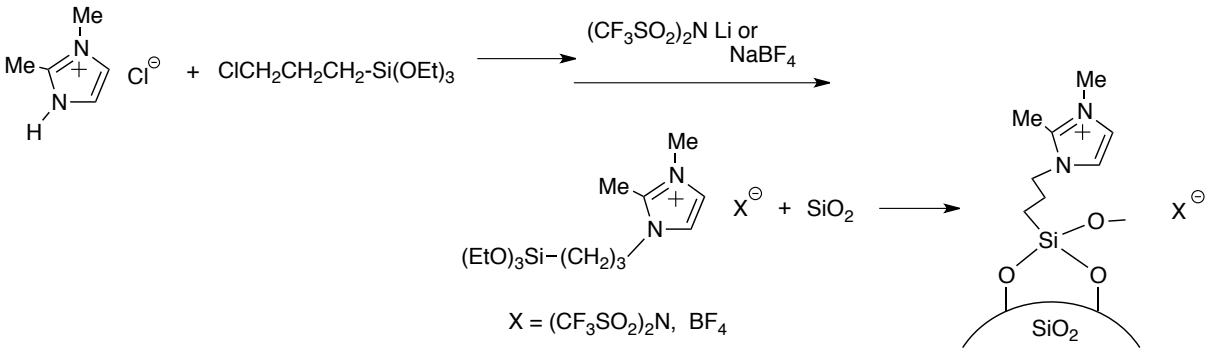

Scheme 1 Immobilization of immidazolium-type ionic liquid onto the silica surface

A similar immobilization of imidazolioum-type ionic liquid has been accomplished through the hydrolysis and condensation with tetraethoxyilane (TEOS) as shown in Scheme 2.[20]

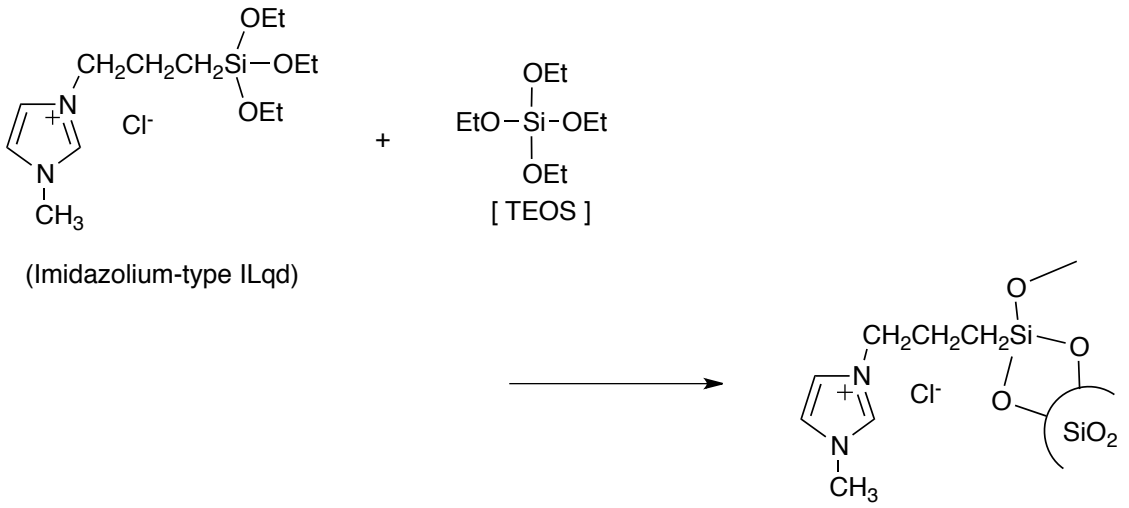

Scheme 2 Immobilization of imidazolium-type ionic liquid onto the silica surface through the hydrolysis and condensation with TEOS

Ionic liquids have been also applied for the useful solvents for the enantioselective acylation.[21] In fact, Itoh et al reported that the lipase-catalyzed enantioselective transesterification of an allylic alcohol can proceed in an ionic liquid such as 1-butyl-3-methylimidazolium hexafluorophosphate as shown in Scheme 3.[21] Of particular interest, it was demonstrated that this reaction is possible to repeatedly use the enzyme in the ionic liquid solvent system. [21]

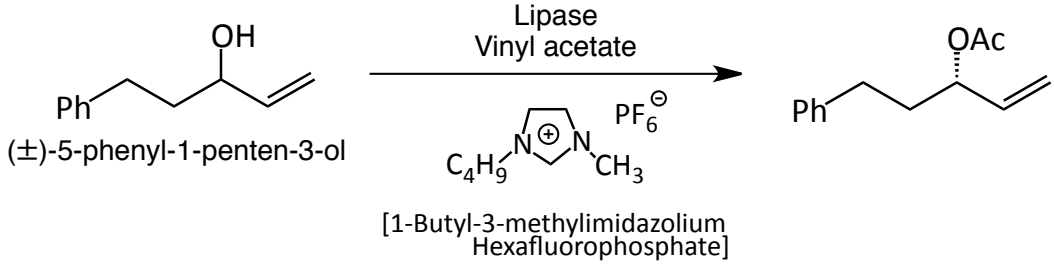

Scheme 3 Lipase-catalyzed enantioselective acylation in the ionic liquid solvent system

TEOS can react with silica nanoparticles in the presence of a variety of ionic liquids such as phosphonium-, ammonium- and imidazolium-type ionic liquids under alkaline conditions to afford the corresponding ionic liquids/silica nanocomposites as shown in Scheme 4.[22] Especially, these ionic liquids/silica nanocomposites can be classified into the nanocomposites possessing no weight loss and weight loss characteristics after calcination at 800 ^{o}C, respectively, according to their structures in the composites.[22] The ionic liquids except for 1-ethyl-3-methylimidazolium hydrogensulfate were found to afford the corresponding ionic liquids/silica nanocomposites possessing no weight loss characteristic even after calcination at 800 ^{o}C.[22]

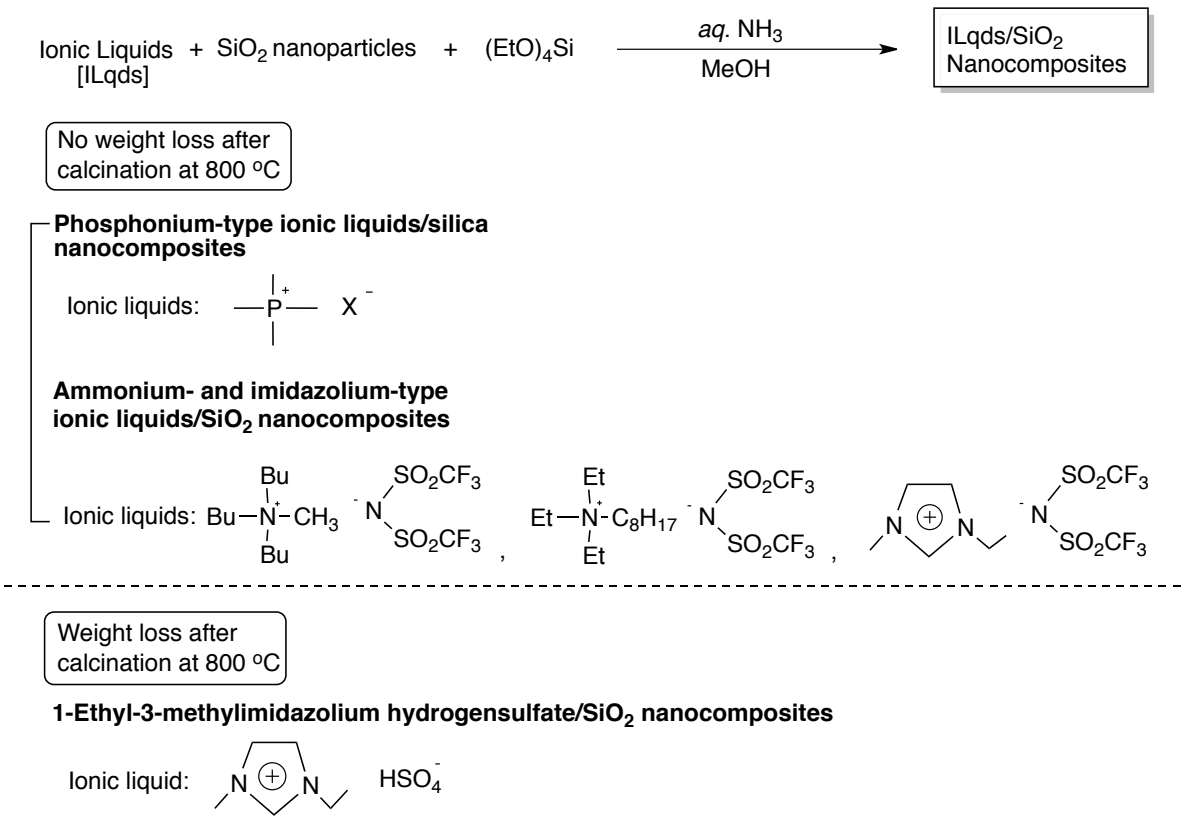

Scheme 4 Preparation of ILqds/SiO2 nanocomposites possessing no weight loss or weightl loss behavior after calcination at 800 °C

The interaction of 1-ethyl-3-methylimidazolium bis(trifluoromethanesulfonyl)amide with silica nanoparticles can afford an ionic liquid gel (ionogel) to give the conductivity equivalent to the corresponding ionic liquid.[23)]

3. Development of polymer/ionic liquids composites

There has been hitherto great interest in a variety of polymerized ionic liquids as polymer electrolytes. For example, vinyl imidazolium-type ionic liquids can undergo the

radical polymerization to afford the corresponding polymers as the polymer-type ionic liquids.[24 ~ 28] However, the ionic conductivity (10^{-7} S/cm level) of the obtained polymers is extremely poor compared with that of the parent monomer (10^{-3} S/cm level) due to the suppression of the migration of cations.[24] Thus, the introduction of the spacer units between the polymerizable moieties and the liquid units enables the resulting polymers to improve the ionic conductivities.[25~ 28]

It is expected that the composite reactions of organic polymers bearing ionic liquid moieties with inorganic molecules could enhance not only the ionic conductivity but also the mechanical strength and thermal stability toward the obtained composite materials. In fact, the radical polymerization of 1-ethyl-4-vinylimidazolium bis(trifluoromethane sulfonyl)imide can proceed with the sol-gel reaction of tetraethoxysilane and trialkoxyboranes under acidic conditions to afford the corresponding organic polymer/inorganic composites illustrated in Scheme 5.[29] The ionic conductivity of the resulting composites was also found to increase compared with that of the parent polymer bearing ionic liquid moieties.[29]

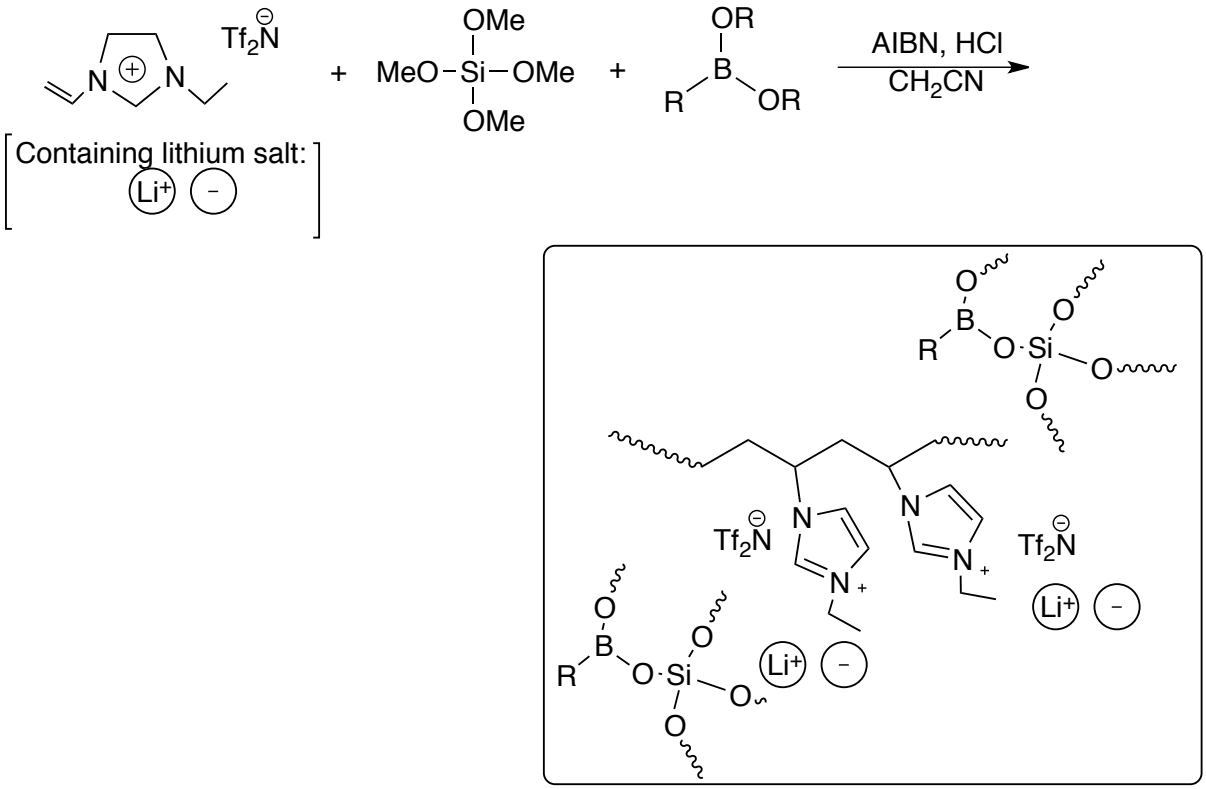

Scheme 5 Preparation of polymers bearing imidazolium moieties/inorganic composites

In addition, from the developmental viewpoints of new organic polymer/ionic liquid composites, ionic liquids such as 1-butyl-3-methylimidazolium hexafluorophosphate and 1-hexyl-3-methylimidazoilium hexafluorophosphate have been applied to the plasticizers for poly(methyl methacrylate), with improved thermal stability.[30] Hitherto, the plasticizer market has been dominated by dioctyl phthalate (DOP); however, there are numerous reports on the health and environmental aspects of the use of DOP.[31] Therefore, the use of ionic liquid for the novel plasticizer will have high potential as an alternate of DOP in the plastic industry.

4 Development of fluorinated polymer/ionic liquid composite materials

As mentioned above**,** ionic liquids are organic salts that are liquid at or near room temperature. Therefore, ionic liquids are non-volatile and non-flammable, and have been hitherto considered to be environmentally friendly alternatives to volatile organic compounds (VOC).[1, 2] Organic compounds are in general poorly soluble in ionic liquids. From the applicable viewpoint of ionic liquids as useful solvents in chemical separations and organic synthesis, studies on the solubilizations of surfactants in ionic liquids including their applications are in particular interest.[2] In fact, it has been already reported that fluorinated polysoaps such as fluoroalkyl end-capped oligomers [R_F-$(M)_n$-R_F; R_F = fluoroalkyl groups, M = radical polymerizable monomers] are effective for the solubilization of fullerene in a variety of ionic liquids.[32] This finding suggests that such fluoroalkyl end-capped oligomers should open a new route for the exploration of novel fluorinated oligomer/ionic liquid composites imparted by both fluorine and ionic liquid. Especially, fluoroalkyl end-capped oligomers can form the nanometer size-controlled self-assembled oligomeric aggregates with the aggregation of terminal fluoroalkyl groups in the oligomers in aqueous and organic media.[33 ~ 36] Interestingly, a wide variety of guest molecules such as carbon nanotube, silica nanoparticles, gold nanoparticles, magnetic nanoparticles, hydroxyapatite, magnesium

carbonate, calcium carbonate, titanium oxide, and organic dyes are smoothly encapsulated into such molecular aggregate cores as guest molecules to provide the corresponding fluorinated oligomeric aggregates/guest molecules nanocomposites as shown in Scheme 6.[37 ~ 69)] Therefore, from the developmental viewpoints of new fluorinated functional materials, it is of particular interest to explore the novel fluorinated oligomeric nanocomposites imparted by ionic liquids.

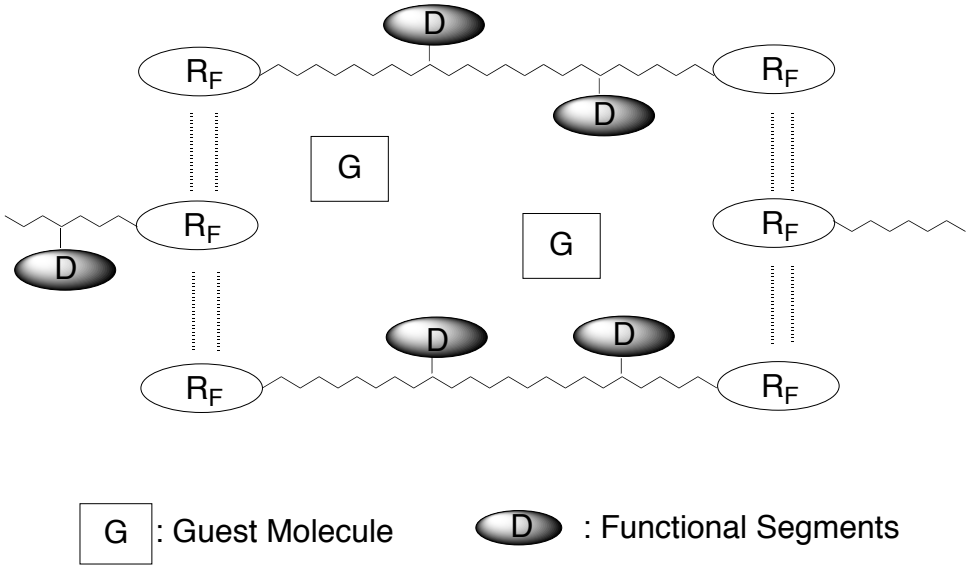

Scheme 6 Schematic illustration for the interaction of self-assembled fluoroalkyl end-capped oligomers $\left[R_F\text{-}(M)_n\text{-}R_F\right.$: R_F ~ $R_F\left.\right]$ with guest molecules

4. Thesis outline

The preparation and applications of a variety of novel fluorinated oligomeric nanocomposites imparted by ionic liquids will be described in this thesis. Chapter 1 demonstrates that the cross-linked fluorinated cooligomeric nanoparticles are applicable to the effective transfer of cytochrome *c* (Cyto-*c*) from aqueous solution to ionic liquids to provide the immobilized Cyto-*c* with the corresponding nanoparticles. The cross-linked fluorinated cooligomeric nanoparticle-encapsulated Cyto-*c* thus obtained are applicable to the oxidation of guaiacol with hydrogen peroxide, and an extremely higher catalytic activity for this oxidation can be observed in the ionic liquid. These results will be also discussed in this Chapter.

Chapter 2 demonstrates on the preparation of new fluoroalkyl end-capped vinyltrimethoxysilane oligomeric silica/ionic liquid nanocomposites by the sol-gel reaction of the corresponding oligomer in the presence of phosphorus-type ionic liquid: tri-*n*-butyl[3-(trimethoxysilyl)propyl]phosphonium chloride under alkaline conditions. These fluorinated nanocomposites thus obtained are applicable to the surface modification of glass, and the modified glass surface can exhibit the superhydrophilicity derived from the hydrophilic cationic ionic liquid segments through the flip-flop motion between fluoroalkyl

groups and the ionic liquid segments in the nanocomposites when the surface environment is changed from air to water. These findings will be also discussed in this Chapter.

Chapter 3 demonstrates that fluoroalkyl end-capped vinyltrimethoxysilane oligomer can undergo the sol-gel reaction under alkaline conditions at room temperature to provide the corresponding fluorinated oligomeric silica nanoparticles, and these fluorinated nanoparticles thus obatined can cause a gelation in a variety of ionic liquids such as phosphonium, ammonium, pyrazolium and imidazolium salts-type ionic liquids. In addition, the modified PMMA [poly(methyl methacrylate)] film treated with these fluorinated oligomeric silica/ionic liquid gels can afford the switching behavior from oleophobic to superhydrophilic characteristics derived from the flip-flop motion between the fluoroalkyl groups and the cationic moieties when the environment on the reverse side is changed from oil to water. These findings will be also discussed in this Chapter.

In Chapter 4, the preparation of the hydrophilic fluoroalkyl end-capped sulfonic acid oligomer/ and fluoroalkyl end-capped sulfobetaine-type oligomer/polyaniline nanocomposites through the polymerization of aniline monomer in the presence of the corresponding oligomers are discussed including their gelling ability of these nanocomposites toward a variety of hydrophilic ionic liquids. Moreover, the ionic conductivity of the obtained fluorinated oligomer/polyaniline/ionic liquid gels will be discussed, compared with that of the

parent ionic liquids.

References

1) T. Welton, *Chem. Rev*., **99**, 2071 (1999).

2) T. Kitazume, T. Fuchigami, H. Sawada, and T. Itoh, "Ionic Liquid - Unreasonable Salt-", Corona Publishing Co., Ltd. (2005).

3) Z. Ma, J. Yu, and S. Dai, *Adv. Mater.,* **22**, 261 (2010).

4) P. Wassercheid and W. Keim, *Angew. Chem. Int. Ed*., **39**, 3772 (2000).

5) J. D. Holbrey and K. R. Seddon, *J. Chem. Soc., Dalton Trans*, 2133 (1999).

6) J. Lu, F. Yan, and J. Texter, *Prog. Polym. Sci*., **34**, 431 (2009).

7) N. Winterton, *J. Mater. Chem*., **16**, 4281 (2006).

8) J. S. Wilkes, *Green Chem*., **4**, 73 (2002).

9) T. Fukushima and T. Aida, *Chem. Eur. J*., **13**, 5048 (2007).

10) J. Dupont, R. F. de Souza, and P. A. Z. Suarez, *Chem. Rev*., **102**, 3667 (2002).

11) D. B. Zhao, M. Wu, Y. Kou, and E. Z. Min, *Catal. Today*., **74**, 157 (2002).

12) V. I. Parvulescu and C. Hardacre, *Chem. Rev*., **107**, 2615 (2007).

13) T. Welton and Coord, *Chem. Rev*., **248**, 2459 (2004).

14) C. P. Mehnert, E. J. Mozeleski, and R. A. Cook, *Chem. Commun*., 3010 (2002).

15) C. P. Mehnert, R. A. Cook, N. C. Dispenziere, and M. Afeworki, *J. Am. Chem. Soc*., **124**, 12932 (2002).

16) B. Orel, A. S. Vuk, V. Jovaovski, R. Jese, L. S. Perse, S. B. Hocevar, E. A. Hutton, B. Ogorevc, and A. Jesih, *Electrochem. Commun*., **7**, 692 (2005).

17) M. H. Valkenberg, C. deCastro, and W. F. Holderich, *Topics in Catalysis*, **14**, 139 (2001).

18) T. P. Nguyen, P. Hesemann, and J. J. E. Moreau, *Microporus Mesoprous Mater*., **142**, 292 (2011).

19) C. Paun, C. Stere, S.M. Coman, V.I. Parvulescu, P. Goodrich, and C. Hardacre, *Catalysis Today*, **131**, 98 (2008).

20) G. Lai, J. Peng, J. Li, H. Qiu, J. Jiang, K.Jiang, and Y. Shen, *Tetrahedron Lett*., **47**, 6951 (2006).

21) T. Itoh, E. Akasaki, K. Kudo, and S. Shirakami, *Chem. Lett*., **30**, 262 (2001).

22) H. Sawada, T. Sasaki, M. Nishida, S. Kodama, and M. Sugiya, *Colloid Polym. Sci*., **290**, 987 (2012).

23) K. Ueno, K. Hata, T. Kataoka, M. Kondoh, and M. Watanabe, *J. Phys. Chem. B*., **112**, 9013 (2008).

24) H. Ohno and K. Ito, *Chem. Lett*., 751 (1998).

25) Y. Yoshizawa and H. Ohno, *Chem. Lett*., 889 (1998).

26) M. Hirao, K. Ito, and H. Ohno, *Electrochim. Acta*., **45**, 1291 (2000).

27) S. Washiro, M. Yoshizawa, H. Nalajima, and H. Ohno, *Polymer*, **45**, 1577 (2004).

28) H. Ohno, M. Yoshizawa, and W. Ogihara, *Electrochim. Acta*, **50**, 225 (2004).

29) T. Mizuno, T. Watanabe, N. Matsumi, and H. Ohno, *Polym. Adv. Technol*., **19**, 1445 (2008).

30) M. P. Scott, M. Rahman, and C. S. Brazel, *Eur. Polym. J.*, **39**, 1947 (2003).

31) B. Hileman, *Chem. Eng. News,* **81**, 33 (2003).

32) H. Sawada and R. Kasai, *Polym. Adv. Technol*., **16**, 655 (2005).

33) H. Sawada, *J. Fluorine Chem*., **105**, 219 (2000).

34) H. Sawada, *J. Fluorine Chem*., **121**, 111 (2003).

35) H. Sawada, *Prog. Polym. Sci*., **32**, 509 (2007).

36) H. Sawada, *Polym. Chem*., **3**, 46 (2012).

37) H. Sawada, Y. Goto, and T. Narumi, *Bull. Chem. Soc. Jpn*., **83**, 82 (2010).

38) H. Takashima, K. Iwaki, K. Takishita, and H. Sawada, *Polym. Adv. Technol*., **20**, 887 (2009).

39) H. Takashima, K. Iwaki, R. Furukuwa, K. Takishita, and H. Sawada, *J. Colloid Interface Sci*., **320**, 436 (2008).

40) Y. Oikawa, T. Saito, S. Idomukai, T. Tanaka, M. Nishida, and H. Sawada, *J. Fluorine Chem*., **177**, 70 (2015).

41) H. Sawada, Y. Shikauchi, H. Kakehi, Y. Katoh, and M. Miura, *Colloid Polym. Sci*., **285**, 499 (2007).

42) T. Saito, H. Kakehi, Y. Kato, M. Miura, N. Isu, and H. Sawada, *Polym. Adv. Technol*., **24**, 532 (2013).

43) T. Saito, M. Nishida, H. Fukaya, H. Kakehi, Y. Kato, M. Miura, N. Isu, and H. Sawada, *Colloid Polym. Sci*., **291**, 945 (2013).

44) H. Sawada, S. Izumi, K. Sasazawa, and M. Yoshida, *J. Colloid Interface Sci*., **377**, 76 (2012).

45) T. Kijima, M. Nishida, H. Fukaya, M. Yoshida, and H. Sawada, *J. Polym. Sci. Part A: Polym. Chem*., **51**, 2555 (2013).

46) M. Mugisawa, K. Ohnishi, and H. Sawada, *Langmuir*, **23**, 5848 (2007).

47) M. Mugisawa and H. Sawada, *Langmuir*, **24**, 9215 (2008).

48) H. Sawada, A. Sasaki, and K. Sasazawa, *Colloid Surf. A: Physicochem. Eng. Aspects*., **337**, 57 (2009).

49) H. Sawada and K. Takahashi, *J. Colloid Interface Sci*., **351**, 166 (2010).

50) H. Sawada, T. Kijima, and M. Mugisawa, *Polymer. J*., **42**, 494 (2010).

51) T. Kijima, I. Javakhishvili, K. Jankova, S. Hvilsted, S. Kodama, M. Sugiya, and H. Sawada, *Colloid Polym Sci*., **290**, 589 (2012).

52) M. Mugisawa, R. Kasai, and H. Sawada, *Langmuir*, **25**, 415 (2009).

53) H. Sawada, T. Narumi, S. Kodama, M. Kamijo, R. Ebara, M. Sugiya, and Y. Iwasaki, *Colloid Polym. Sci*., **285**, 977 (2007).

54) H. Sawada, T. Tashima, Y. Nishiyama, M. Kikuchi, G. Kostov, Y. Goto, and B. Ameduri, *Macromolecules*, **44**, 1114 (2011).

55) H. Sawada, M. Kikuchi, and M. Nishida, *J. Polym. Sci. Part A; Polym. Chem*., **49**, 1070 (2011).

56) H. Sawada, T. Tashima, H. Kakehi, Y. Nishiyama, M. Kikuchi, M. Miura, Y. Sato, and N. Isu, *Polym. J*., **42**, 167 (2010).

57) H. Sawada, T. Tashima, and S. Kodama, *Polym. Adv. Technol*., **19**, 739 (2008).

58) H. Sawada, H. Kakehi, T. Tashima, Y. Nishiyama, M. Miura, and N. Isu, *J. Appl. Polym. Sci*., **112**, 3482 (2009).

59) H. Sawada, X. Liu, Y. Goto, M. Kikuchi, T. Tashima, and M. Nishida, *J. Colloid Interface Sci*., **356**, 8 (2011).

60) S. Soma, Y. Mizutani, M. Sugiya, and H. Sawada, *J. Polym. Sci., Part A: Polym. Chem.*, **52**, 1869 (2014).

61) H. Sawada, Y. Matsuki, Y. Goto, S. Kodama, M. Sugiya, and Y. Nishiyama, *Bull. Chem. Soc. Jpn*., **83**, 75 (2010).

62) Y. Aomi, M. Nishida, and H. Sawada, *J. Polym. Sci., Part A: Polym. Chem*., in press.

63) H. Sawada, E. Sawada, H. Kakehi, T. Kariya, M. Mugisawa, Y. Chounan, M. Miura, and N. Isu, *Polym. Compos*., **30**, 1848 (2009).

64) E. Sawada, H. Kakehi, Y. Chounan, M. Miura, Y. Sato, N. Isu, and H. Sawada, *Composites Part B*, **41**, 498 (2010).

65) S. Guo, H. Yoshioka, H. Kakehi, Y. Kato, M. Miura, N. Isu, B. Ameduri, and H. Sawada, *J. Colloid Interface Sci*., **387**, 141 (2012).

66) S. Guo, H. Yoshioka, Y. Kato, H. Kakehi, M. Miura, N. Isu, A. Manseri, H. Sawada, and B. Ameduri, *Eur. Polym. J*., **58**, 79 (2014).

67) S. Guo, S. Soma, K. Okuno, T. Saito, T. Nakagawa, K. Sato, and H. Sawada, *Composites: Part B*, **70**, 80 (2015).

68) S. Guo, T. Ogasawara, T. Saito, H. Kakehi, Y. Kato, M. Miura, N. Isu, and H. Sawada, *Colloid Polym. Sci*., **291**, 2947 (2013).

69) H. Sawada, T. Tsuzuki-ishi, T. Kijima, J. Kawakami, M. Iizuka, and M. Yoshida, *J. Colloid Interface Sci*., **359**, 461 (2011).

CHAPTER 1

Preparation of Novel Cross-linked Fluoroalkyl End-capped Cooligomeric Nanoparticles-Encapsulated Cytochrome *c* in Water and Ionic Liquids

1.1. Introduction

Room-temperature ionic liquids (ILqds) as green solvents have been recently applied in a wide variety of fields such as organic syntheses[1 ~ 4], extraction/separation[5, 6], battery electrolytes[7 ~ 10], capacitor[11, 12], and polymer chemistry[13 ~ 15], due to exhibiting unusual features such as nonvolatility, thermal stability, electrochemical stability, and high ion conductivity, which cannot be achieved in the conventional organic solvents. Organic solvents are usually used in the extraction/separation of biomaterials based on reverse micelles and microemulsions.[16, 17] In contrast, ILqds are reported to be attractive matrix for biomaterials[18], and in fact, ILqds have been used in extraction/separation of biological molecules as the alternative solvents of traditional volatile organic solvents. For example, Goto et al.[19, 20] and Hong et al.[21], individually, reported the extraction of cytochrome *c* (Cyto-*c*) from aqueous solution into ILqds. Crown ethers are usually used as coexisting extractants/additive in these extraction systems[19, 20]; however, studies on the exploration of effective extractants in such systems have been hitherto very limited except for crown ethers. During the comprehensive studies on the development of novel extractants possessing a higher surface-activity as well as crown ethers[22, 23], it has been already reported that fluoroalkyl end-capped *N*-(1,1-dimethyl-3-oxobutyl)acrylmide oligomer [R_F-(DOBAA)$_n$-R_F] can interact

with Cyto-*c* to afford the immobilized Cyto-*c*.[24] This makes it interesting to study the interaction of fluoroalkyl end-capped oligomers with Cyto-*c* not only in water but also in ILqds. This Chapter demonstrates that the cross-linked fluoroalkyl end-capped acrylic acid cooligomer containing poly(oxyethylene) units can interact smoothly with Cyto-*c* in not only water but also ILqds to afford the novel fluorinated cooligomeric nanoparticles-encapsulated Cyto-*c* in these solvents.

1.2. Experimental

1.2.1. Measurements

Ultraviolet-visible (UV-vis) spectra were measured by using Shimadzu UV-1600 UV-vis spectrophotometer (Kyoto, Japan). Dynamic light-scattering (DLS) were measured by using Otsuka Electronics DLS-7000 HL (Tokyo, Japan). Scanning electron microscopy (SEM) images were measured by using JEOL JSM-5300 (Tokyo, Japan).

1.2.2. Materials

Acrylic acid (ACA) and dimethacrylate monomer containing poly(oxyethylene) units were used as received from Toagosei Co., Ltd. (Tokyo, Japan) and NOF corporation (Tokyo, Japan), respectively. Cytochrome *c* from horse heart (MW = 12,350) was purchased from Wako Pure Chemical Industries Ltd. (Osaka, Japan). 1-Ethyl-3-methylimidazolium bis(trifluoromethanesulfonyl)imide, 1-butyl-3-methylimidazolium bis(trifluoromethane-sulfonyl)imide, and 3-methylpyrazolium tetrafluoroborate were purchased from Kanto Chemical Co., Ltd. (Tokyo, Japan), Toyo Gosei Co., Ltd. (Chiba, Japan), and Stella Chemifa Co., Ltd. (Osaka, Japan), respectively.

Cross-linked fluoroalkyl end-capped acrylic acid cooligomer containing poly(oxyethylene) units [R_F-(PDE-100)$_x$-(ACA)$_y$-R_F; R_F = $CF(CF_3)OC_3F_7$] was prepared by the reaction of acrylic acid and dimethacrylate monomer containing poly(oxyethylene) units according to the previously reported method.[25)]

1.2.3. Liquid-liquid extraction of Cyto-*c* into ILqds

A typical experiment for liquid-liquid extraction of Cyto-*c* into ILqds is as follows: 2 ml

of Cyto-*c* (from horse heart: 2 mg) aqueous solution and 2 ml of R_F-(PDE-100)$_x$-(ACA)$_y$-R_F cooligomer (16 mg) ionic liquid [1-ethyl-3-methylimidazolium bis(trifluoromethanesulfonyl)-imide; EMI-TFSI] solution were mixed, and stirred at 5 ^oC for 3 h. After being left to stand 24 h at 5 ^oC, immobilized Cyto-*c* with R_F-(PDE-100)$_x$-(ACA)$_y$-R_F cooligomer precipitated and was collected by quantitative yield (~ 100 %). No Cyto-*c* [λ_{max}: 408 nm: see Fig. 1-3(b), and (c)] was detected in either the aqueous or ILqds phases by UV-vis spectroscopy. In addition, this immobilized Cyto-*c* was able to disperse into the parent ILqds to afford the well-dispersed R_F-(PDE-100)$_x$-(ACA)$_y$-R_F cooligomeric nanoparticles-encapsulated Cyto-*c*, quantitatively [see Fig. 1-3-(d)].

1.2.4. Guaiacol oxidation with fluorinated cooligomeric nanoparticles-encapsulated Cyto-*c*

2 ml of cytochrome *c* from horse heart (MW = 12,350; 2 mg) solution in 0.07 M phosphate buffer (pH 6.9) and 2 ml of a 1,2-dichloroethane solution of R_F-(DOBAA)$_n$-R_F oligomer [R_F = $CF(CF_3)OCF_2CF(CF_3)OC_3F_7$: 16 mg] were placed in a 10 ml vial and shaken vigorously for 20 min at 25 ^oC. After being left to stand 24 h at 5 ^oC, immobilized cytochrome *c* (Cyto-*c*) with R_F-(DOBAA)$_n$-R_F oligomer precipitated and was collected by

simple filtration. The immobilized Cyto-*c* [R_F-(DOBAA)$_n$-R_F/Im-Cyto-*c*; R_F = $CF(CF_3)OCF_2CF(CF_3)OC_3F_7$] thus obtained was added to the phosphate buffer solution (pH 6.9: 2 ml). To this buffer solution guaiacol (37 μmol) and hydrogen peroxide (3 μmol) were added, and the obtained mixture was stirred at 5 ^oC for 30 minutes to detect the increase of the absorbance at around 470 nm related to the guaiacol oxidation product by using the UV-vis spectral measurements. The guaiacol oxidation with the well dispersed aqueous solution containing R_F-(PDE-100)$_x$-(ACA)$_y$-R_F cooligomeric nanoparticles-encapsulated Cyto-*c* and the homogeneous R_F-(PDE-100)$_x$-(ACA)$_y$-R_F cooligomer/Cyto-*c* nanocomposite solutions [mixed solvents of water and 3MP-BF4 (vol., 1/1)] were studied under similar conditions.

1.3. Results and discussion

Cross-linked fluoroalkyl end-capped acrylic acid cooligomer containing poly(oxyethylene) units [R_F-(PDE)$_x$-(ACA)$_y$-R_F], which was prepared by the reaction of acrylic acid and dimethacrylate monomer containing poly(oxyethylene) units (see Scheme 1-1), can form the corresponding cross-linked cooligomeric nanoparticles (average particle size determined by dynamic light scattering (DLS) measurements: 361 ± 63 nm) in water.

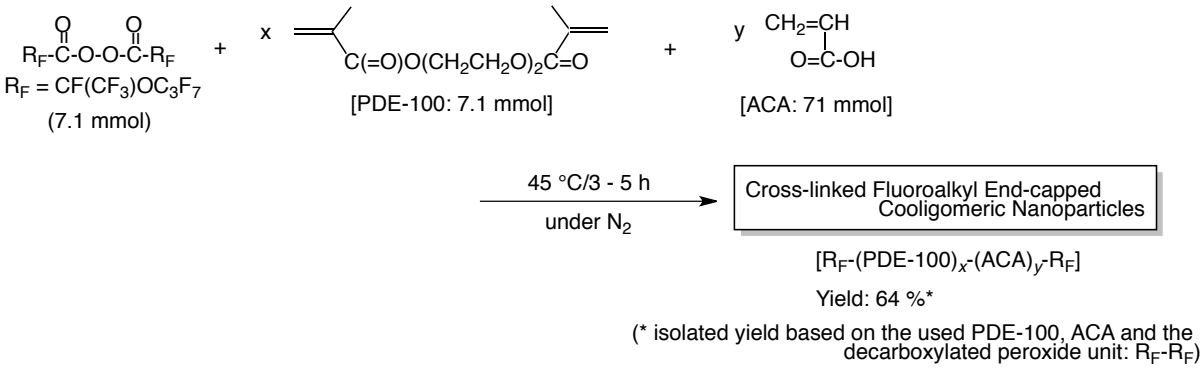

Scheme 1-1 Preparation of cross-linked fluorinated cooligomeric nanoparticles

In general, cross-linking of fluorinated polymers such as vinylidene fluoride-containing polymer with a dehydrofluorination process has been already reported by Ameduri et al..[26] However, a simple cross-linking reaction through a radical process illustrated in Scheme 1-1 is very convenient for the preparation of the expected fluorinated cooligomeric nanoparticles under mild conditions. The aqueous solution (2 ml) containing cross-linked R_F-(PDE)$_x$-(ACA)$_y$-R_F cooligomer (16 mg) was added into an aqueous solution (2 ml) of Cyto-*c* (2 mg), and was stirred at 5 ^oC for 3 hr. After stirring, R_F-(PDE)$_x$-(ACA)$_y$-R_F/Cyto-*c* nanocomposites were quantitatively isolated after the simple centrifugal separation (2000 rpm/20 min), and the encapsulated ratio of Cyto-*c* into fluorinated nanoparticles was estimated to be 90 % by UV-vis spectra measurements (λ_{max}: 408 nm, see Fig. 1-1).

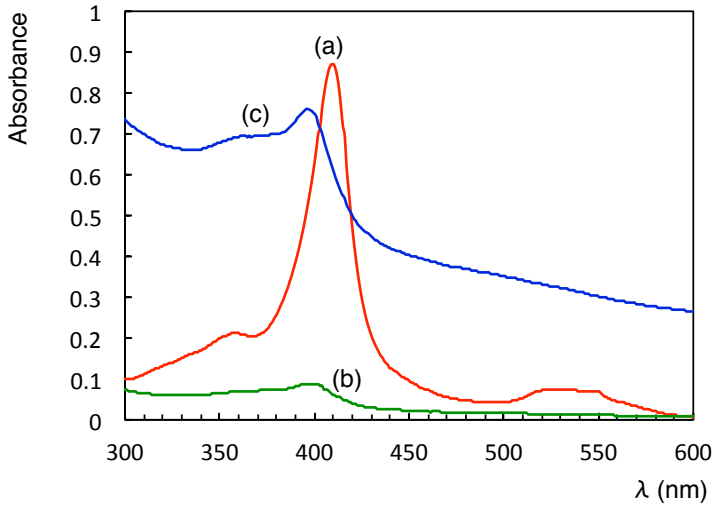

Fig. 1-1 UV-vis spectra of R_F-(PDE-100)$_x$-(ACA)$_y$-R_F nanoparticles-encapsulated Cyto-*c* in aqueous solutions.

(a) Cyto-*c* (1.0 g/dm^3) in aqueous solution.
(b) Supernatant solution after centrifugal separation.
(c) Redispersed R_F-(PDE-100)$_x$-(ACA)$_y$-R_F nanoparticles-encapsulated Cyto-*c* in aqueous solution.

This isolated nanocomposite was found to afford a good re-dispersibility in water, and the well-dispersed composite solution afforded a slightly blue-shifted absorption from 408 nm (parent Cyto-*c*) to 396 nm [see Fig. 1-1(a), and (c)] indicating that Cyto-*c* was effectively encapsulated into the fluorinated nanoparticle cores as a guest molecule. The size (33.7 ± 4.0 nm) of the re-dispersed fluorinated nanoparticles-encapsulated Cyto-*c* was effectively decreased by the encapsulation of Cyto-*c*, compared to that (361 nm) of the parent fluorinated cooligomeric nanoparticles. The decrease of the size of nanoparticles indicates that the encapsulation of Cyto-*c* could proceed smoothly to yield fine fluorinated cooligomeric nanoparticles-encapsulated Cyto-*c* with around 30 nm levels. The SEM (scanning electron

microscopy) photography of aqueous solution of fluorinated nanoparticles-encapsulated Cyto-*c* has been measured, and the result is shown in Fig. 1-2.

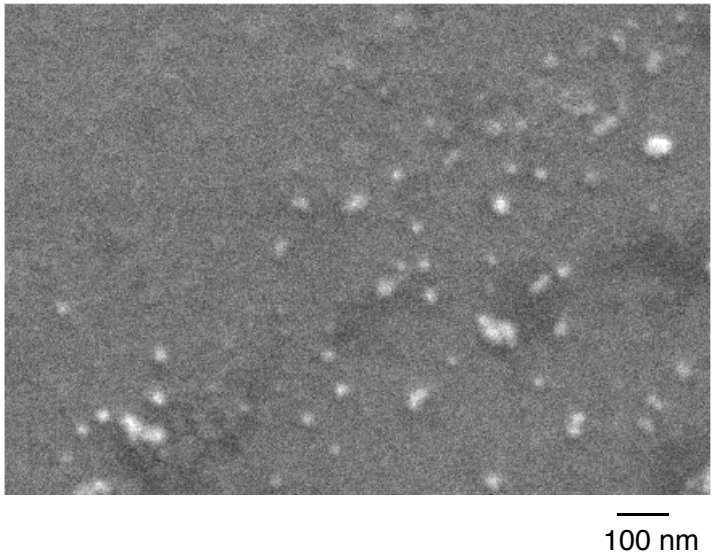

Fig. 1-2 Scannin electron microscopy (SEM) image of R_F-(PDE-100)$_x$-(ACA)$_y$-R_F nanoparticles-encapsulated Cyto-*c* in Water.

The electron micrograph also shows the formation of cross-linked fluorinated cooligomeric nanoparticles-encapsulated Cyto-*c* with a mean diameter of 31 nm, of whose value is the same as that (34 nm) of DLS measurements.

Interestingly, the present cross-linked R_F-(PDE)$_x$-(ACA)$_y$-R_F cooligomeric nanoparticles were found to exhibit a good solubility in ILqds such as 1-ethyl-3-methylimidazolium bis(trifluoromethanesulfonyl)imide [EMI-TFSI], 1-butyl-3-methylimidazolium bis(trifluoro-methanesulfonyl)imide [BMI-TFSI] and 3-methylpyrazolium tetrafluoroborate [3MP-BF4].

Thus, the extraction of Cyto-*c* (2 mg) was tried from aqueous phase (2 ml) into EMI-TFSI (2 ml) with the R_F-$(PDE)_x$-$(ACA)_y$-R_F cooligomeric nanoparticles (16 mg), and the results are shown in Fig. 1-3.

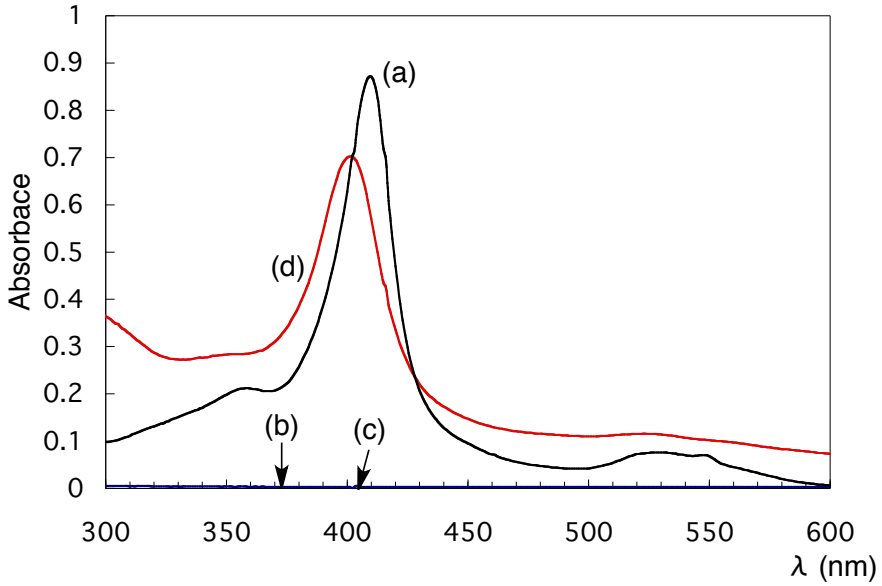

Fig. 1-3 UV-vis spectra of redispersed R_F-$(PDE\text{-}100)_x$-$(ACA)_y$-R_F nanoparticles-encapsulated Cyto-*c* in EMI-TFSI.

(a) Cyto-*c* (1.0 g/dm^3) in aqueous solution.
(b) Aqueous phase after collection of immobilized Cyto-*c*.
(c) EMI-TFSI phase after collection of immobilized Cyto-*c*.
(d) Dispersed R_F-$(PDE\text{-}100)_x$-$(ACA)_y$-R_F nanoparticles-encapsulated Cyto-*c* in EMI-TFSI.

As shown in Fig. 1-3, it was demonstrated that R_F-$(PDE)_x$-$(ACA)_y$-R_F nanoparticles can afford the immobilized Cyto-*c*, quantitatively, to afford no absorption peak related to Cyto-*c* in aqueous or EMI-TFSI phases after the simple liquid-liquid extraction assay. Interestingly, this immobilized Cyto-*c* with R_F-$(PDE)_x$-$(ACA)_y$-R_F cooligomeric nanoparticles has a good

dispersibility in the parent ionic liquid (EMI-TFSI) to afford the homogeneous ionic liquid solutions containing R_F-(PDE)$_x$-(ACA)$_y$-R_F cooligomeric nanoparicles-encapsulated Cyto-*c*, quantitatively [see Fig. 1-3(d)]. In fact, DLS measurements show that the size of the dispersed fluorinated cooligomer/Cyto-*c* composites in EMI-TFSI was found to decrease effectively from 245 ± 62 nm (the size of parent fluorinated cooligomeric nanoparticles in EMI-TFSI) to 32.5 ± 7.4 nm, indicating that the present immobilized Cyto-*c* can afford the nanometer size-controlled fluorinated Cyto-*c* composites in EMI-TFSI. A slightly blue-shifted absorption from 409 to 396 nm of the obtained composites [see Fig. 1-3(a), and (d)] also shows that Cyto-*c* should be tightly encapsulated into fluorinated nanoparticle cores.

On the other hand, unexpectedly, the immobilized Cyto-*c* could not be isolated by the use of 3MP-BF4 under the similar conditions in Fig. 1-3. However, the homogeneous R_F-(PDE-100)$_x$-(ACA)$_y$-R_F cooligomer/Cyto-*c* nanocomposite solutions (the size of this composite: 31.2 ± 7.3 nm in 3MP-BF4 and the size of the parent fluorinated cooligomeric nanoparticles: 241 ± 60 nm in 3MP-BF4) were obtained as shown in Fig. 1-4. This finding would be due to the higher hydrophilic characteristic of 3MP-BF4.

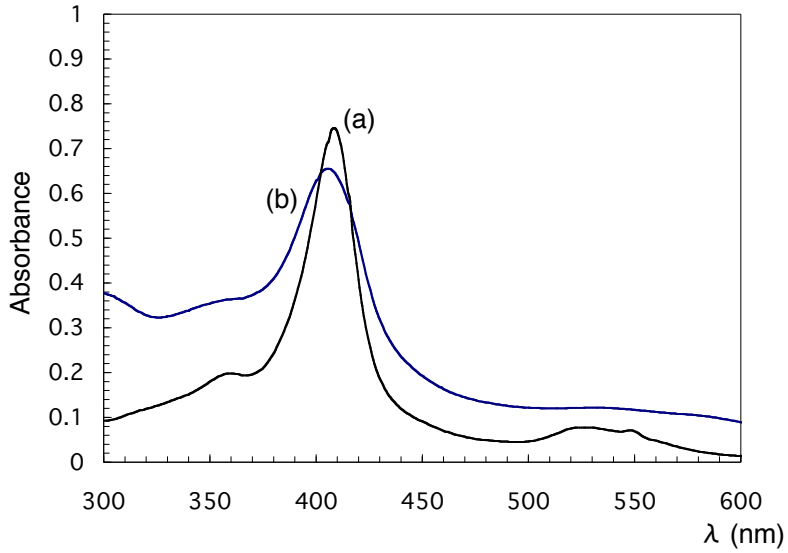

Fig. 1-4 UV-vis spectra of R_F-(PDE-100)$_x$-(ACA)$_y$-R_F nanoparticles-encapsulated Cyto-*c* in mixed solvents [water and 3MP-BF4 (vol., 1/1)].

(a) Cyto-*c* (1.0 g/dm^3) in aqueous solution.

(b) R_F-(PDE-100)$_x$-(ACA)$_y$-R_F nanoparticles-encapsulated Cyto-*c* in mixed solvents [water and 3MP-BF4].

Hitherto, it is well known that Cyto-*c* is applicable to the oxidation reaction of guaiacol, and the oxidation mechanism is considered to proceed through the compound A and compound B intermediates as illustrated in Scheme 1-2.[27, 28)]

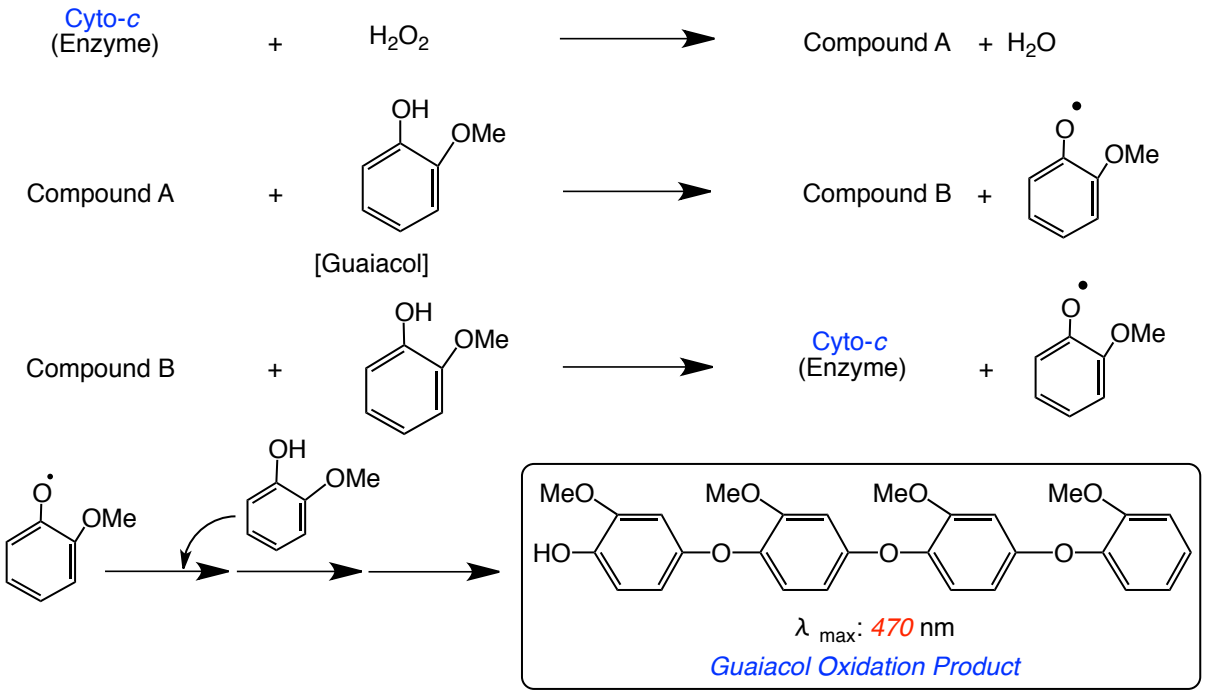

Scheme 1-2 Possible reaction mechanism for the oxidation of guaiacol with hydrogen peroxide catalysed by Cyto-*c*.

Thus, to test whether the cross-linked R_F-$(PDE)_x$-$(ACA)_y$-R_F cooligomeric nanoparticles-encapsulated Cyto-*c* retain its enzyme catalytic activity, Cyto-*c* - dependent guaiacol oxidation with hydrogen peroxide was studied according to the previously reported method (reaction conditions: 25 °C for 30 min).[24] It has been already reported that fluoroalkyl end-capped *N*-(1,1-dimethyl-3-oxobutyl)acrylamide oligomer [R_F-$(DOBAA)_n$-R_F] can immobilize Cyto-*c* through the liquid (water) - liquid (1,2-dichloroethane) extraction technique.[24] The immobilized Cyto-*c* [R_F-$(DOBAA)_n$-R_F/Im-Cyto-*c*; R_F = $CF(CF_3)OCF_2$-$CF(CF_3)OC_3F_7$] was applied to the oxidation reaction of guaiacol in the presence of hydrogen peroxide to afford the corresponding product at around λ_{max}: 470 nm, for comparison. The

obtained immobilized Cyto-*c* [R_F-(DOBAA)$_n$-R_F/Im-Cyto-*c*; R_F = $CF(CF_3)OCF_2CF(CF_3)O$-C_3F_7] can also exhibit its catalytic activity for oxidation of guaicoal with hydrogen peroxide under the similar conditions, and the guaiacol oxidation product ratio was also demonstrated, for comparison. These results are shown in Table 1-1.

Table 1-1 Guaiacol oxidation with R_F-oligomers/Cyto-*c* nanocomposites

Nanocomposites[a]	Solvent	λ_{max} (nm)	Guaiacol oxidation product based on R_F-(DOBAA)$_n$-R_F/Im-Cyto-*c*
R_F-(DOBAA)$_n$-R_F/Im-Cyto-*c*[b]	Water	470	1.00
R_F-(PDE-100)$_x$-(ACA)$_y$-R_F/Cyto-*c*[c]	Water	493	1.24
R_F-(PDE-100)$_x$-(ACA)$_y$-R_F/Cyto-*c*[d]	Mixed solvents of water and 3MP-BF_4(vol., 1/1)	485	*28.3*

a) Used R_F-(DOBAA)$_n$-R_F oligomer (or R_F-(PDE-100)$_x$-(ACA)$_y$-R_F cooligomer), 16 mg; used Cyto-*c*, 2 mg; and used hydrogen peroxide, 3 μmol.
b) Immobilization ratio of Cyto-*c*, 93%.
c) Encapsulation ratio of Cyto-*c*, 90%.
d) Encapsulation ratio of Cyto-*c*, 100%.

The addition of hydrogen peroxide to the aqueous solutions of guaiacol containing cross-linked fluorinated cooligomeric nanoparticles-encapsulated Cyto-*c* was found to initiate guaiacol oxidation to increase absorbance around 485 ~ 493 nm related to oxidized guaiacol at 25 ^oC. Interestingly, R_F-(PDE)$_x$-(ACA)$_y$-R_F cooligomeric nanoparticles-encapsulated Cyto-*c* exhibited more effective enzyme catalytic activity than that of R_F-(DOBAA)$_n$-R_F/Im-Cyto-*c* in aqueous solutions. Unexpectedly, R_F-(PDE-100)$_x$-(ACA)$_y$-R_F cooligomer/Cyto-*c*

nanocomposites [see Fig. 1-4(b)] were found to be the most active for the guaiacol oxidation with hydrogen peroxide: 28.3-fold relative to that of R_F-(DOBAA)$_n$-R_F/Im-Cyto-*c*, indicating that cross-linked R_F-(PDE-100)$_x$-(ACA)$_y$-R_F cooligomeric nanoparticles would specifically bind Cyto-*c* in the nanoparticle cores through not only an electrostatic interaction of a positive charge at the entrance of the hydrophobic Cyto-*c* channel but also an electrostatic interaction with ionic liquid (3MP-BF4) to afford the extremely higher enzyme catalytic activity in the guaiacol oxidation with hydrogen peroxide.[29)]

1.4. Conclusion

In summary, cross-linked fluorinated cooligomeric nanoparticles were able to interact with Cyto-*c* in water to afford the corresponding nanoparticles-encapsulated Cyto-*c*, effectively. The fluorinated nanocomposites were also easily isolated by the simple centrifugal separation, and the isolated powder can be effectively re-dispersed into water to afford the nanometer size-controlled fluorinated cooligomeric nanoparticles-encapsulated Cyto-*c*. Similarly, this fluorinated cooligomeric nanoparticle can interact with Cyto-*c* in ILqds to afford the corresponding fluorinated cooligomer/Cyto-*c* nanocomposites. These fluorinated cooligomer/Cyto-*c* nanocomposites thus obtained in water and ILqds were found

to exhibit enzyme catalytic activity for the guaiacol oxidation with hydrogen peroxide.

References

1) T. Welton, *Chem. Rev*., **99**, 2071 (1999).

2) C. E. Song and E. J. Roh, *Chem. Commun*., 837 (2000).

3) Y. S. Vygodskii, E. I. Lozinskaya, A. S. Shaplov, K. A. Lyssenko, M. Y. Antipin, and Y. G. Urman, *Polymer*, **45**, 5031 (2004).

4) N. Jain, A. Kumar, S. Chauhan, and S. M. S. Chauhan, *Tetrahedron*, **61**, 1015 (2005).

5) J. G. Huddleston, H. D. Willauer, R. P. Swatloski, A. E. Visser, and R. D. Rogers, *Chem. Commun*., 1765 (1998).

6) J. H. Wang, D. H. Cheng, X. W. Chen, Z. Du, and Z. L. Fang, *Anal. Chem*., **79**, 620 (2007).

7) N. Nishimura and H. Ohno, *J. Mater. Chem*., **12**, 2299 (2002).

8) A. M. Leone, S. C. Weatherly, M. E. Williams, H. H. Thorp, and R. W. Murray, *J. Am. Chem. Soc*., **123**, 218 (2001).

9) H. Sakaeba and H. Matsumoto, *Electrochem. Commun*., **5**, 594 (2003).

10) R. Kawano and M. Watanabe, *Chem. Commun*., 330 (2002).

11) M. Ue, M. Takeda, T. Takahashi, and M. Takehara, *Electrochem. Solid-State Lett.*, **5**, A119 (2002).

12) A. B. McEwen, S. F. McDevitt, and V. R. Koch, *J. Electrochem. Soc.*, **144**, L84 (1997).

13) T. Biedron and P. Kubisa, *J. Polym. Sci.: Part A: Polym. Chem.*, **40**, 2799 (2002).

14) H. Zhang, K. Hong, and J. W. Mays, *Macromolecules*, **35**, 5738 (2002).

15) S. Perrier, T. P. Davis, A. J. Carmichael, and D. M. Haddleton, *Chem. Commun*., 2226 (2002).

16) T. Ono, M. Goto, F. Nakashio, and T. A. Hatton, *Biotechnol. Prog*., **12**, 793 (1996).

17) M. Vasudevan and J. M. Wiencek, *Ind. Eng. Chem. Res*., **35**, 1085 (1996).

18) H. Ohno, C. Suzuki, and K. Fujita, *Electrochimica Acta*, **51**, 3685 (2006).

19) K. Shimojo, K. Nakashima, N. Kamiya, and M. Goto, *Biomacromolecules*, **7**, 2 (2006).

20) K. Shimojo, N. Kamiya, F. Tani, H. Naganawa, Y. Naruta, and M. Goto, *Anal. Chem.,* **78**, 7735 (2006).

21) C. D.-Hong, C. X.-Wei, S. Yang, and W. J.-Hua, *Chin. J. Anal. Chem*., **36**, 1187 (2008).

22) H. Sawada, *Prog. Polym. Sci*., **32**, 509 (2007).

23) H. Sawada, *Polym. J.,* **39**, 637 (2007).

24) H. Sawada, Y. Hirata, T. Kawase, and K. Fujimori, *J. Fluorine Chem*., **106**, 73 (2000).

25) H. Yoshioka, T. Narumi, and H. Sawada, *J. Oleo Sci*., **56**, 377 (2007).

26) A. Taguet, B. Ameduri, and B. Boutevin, *Adv. Polym. Sci*., **184**, 127 (2005).

27) B. Chance and A. C. Maehly, "*Methods in Enzymology*", S. Colowick and N. O. Kaplan eds., Vol 2., pp764, Academic Press (1955).

28) S. Marklund, P. –I. Ohlsson, A. Opera, and K. –G. Paul, *Biochim. Biophys. Acta*., **350**, 304 (1974).

29) M. Rytomaa and P. K. J. Kinnunen, *J. Biol. Chem.*, **270**, 3197 (1995).

CHAPTER 2

Application of Ionic Liquid as Surface Modifier: Switching Behavior of Novel Fluoroalkyl End-capped Vinytrimethoxysilane Oligomer – Tri-*n*-butyl[3-(trimethoxysilyl)propyl]phosphonium Chloride Silica Nanocomposites between Superhydrophilicity and Oleophobicity

2.1. Introduction

Ionic liquids (ILqds) have been widely applied as recyclable alternatives to conventional organic solvents for chemical synthesis and liquid-liquid extractions, catalyst, electrochemistry, and analytics, because they can exhibit negligible vapor pressure, high chemical and thermal stabilities, and high ionic conductivities.[1 ~ 12)] Interestingly, ILqds have been applied to the architecture of smart surfaces with their counter anion-responsiveness to exhibit their hydrophilicity and hydrophobicity by simply exchanging counter anions.[13 ~ 15)] Thus, utilization of this switching behavior opens a new way to control the properties of the material surface.[16 ~ 20)] On the other hand, fluoroalkyl end-capped oligomers are attractive functional materials because they exhibit a variety of unique properties such as high solubility, surface active properties, biological activities, and nanometer size-controlled self-assembled molecular aggregates which cannot be achieved by the corresponding non-fluorinated and randomly fluoroalkylated ones.[21 ~ 24)] Especially, it has been already reported that fluoroalkyl end-capped oligomers are potential surface modifiers for not only inorganic materials such as glasses, stainless steel and aluminum plate but also traditional organic polymers such as polystyrene and poly(methyl methacrylate) to exhibit a good oleophobicity imparted by fluorocarbon.[25 ~ 28)] Thus, it is strongly expected that the introduction of hydrophilic ILqds

into fluoroalkyl end-capped oligomers should exhibit a switchable wettability between the oleophobicity imparted by fluorocarbon and hydrophilicity derived from ILqds through the flip-flop motion between fluoroalkyl groups and ILqds segments in fluorinated oligomers adapting to the surface environmental changes. Here, this Chapter shows that novel fluoroalkyl end-capped vinyltrimethoxysilane oligomer - tri-*n*-butyl[3-(trimethoxysilyl)-propyl]phosphonium chloride [TBSiPCl]/silica nanocomposites can be prepared by the sol-gel reaction of the corresponding oligomer in the presence of TBSiPCl under alkaline conditions. The modified glass surface treated with these nanocomposites can also exhibit a strong oleophobicity imparted by fluoroalkyl segments in the composites. More interestingly, it was verified that the modified glass surface exhibits the switching behavior between the oleophobic and superhydrophilic characteristics adapting to the environmental changes on the modified surface. This is a first example for the application of ionic liquids to the fluorinated polymeric modifiers. These results will be described in this Chapter.

2.2. Experimental

2.2.1. Measurements

Fourier-transform infrared (FTIR) spectra were measured using Shimadzu FTIR-8400 FT-IR spectrophotometer (Kyoto, Japan). The contact angles were measured by the use of Kyowa Interface Science Drop Master 300 (Saitama, Japan) on the modified glass surface. Scanning electron microscopy (SEM) images were measured by using JEOL JSM-5300 (Tokyo, Japan). DFM (Dynamic Force Mode) was measured by using SII NanoTechnology Inc. E-sweep (Chiba, Japan).

2.2.2. Materials

Tri-*n*-butyl-[3-(trimethoxysilyl)propyl]phosphonium chloride was received from Nippon Chemical Industrial Co., Ltd., Tokyo, Japan. Vinyltrimethoxysilane (VM) was used as received from Dow Corning Toray Co., Ltd. (Tokyo, Japan). Fluoroalkyl end-capped vinyltrimethoxysilane oligomer was prepared by reaction of fluoroalkanoyl peroxide with the corresponding monomer according to the previously reported method.[29)]

2.2.3. Preparation of fluoralkyl end-capped viniyltrimethoxysilane oligomer – ionic liquid silica nanocomposites

A typical procedure for the preparation of fluoroalkyl end-capped vinyltrimethoxysilane oligomer – ionic liquid silica nanocomposites is as follows: To methanol solution (20 ml) containing fluoroalkyl end-capped vinyltrimethoxysilane oligomer [100 mg; R_F-[$CH_2CHSi(OMe)_3$]$_n$-R_F: R_F-$(VM)_n$-R_F; R_F = $CF(CF_3)OC_3F_7$; n = 2 ~ 3] and tri-*n*-butyl-[3-(trimethoxysilyl)propyl]phosphonium chloride (0.9 ml), was added 25 % aqueous ammonia solution (5 ml). The mixture was stirred with a magnetic stirring bar at room temperature for 2 hr. After centrifugal separation of this solution, the obtained products were well washed with methanol, and dried in vacuo to afford the expected white powdery product (630 mg). The expected product [R_F-$(VM)_n$-R_F/TBSiPCl/SiO_2 nanocomposites] thus obtained was subsequently characterized by the use of FT-IR [ν/cm^{-1}: 2959 (CH), 1335 (CF_3), 1242 (CF_2), 1103 (Si-O-Si)].

2.2.4. Surface modification of glass with R_F-$(VM)_n$-R_F/TBSiPCl/SiO_2 nanocomposites

The methanol solution (20 ml) containing fluoroalkyl end-capped vinyltrimethoxysilane

oligomer (100 mg), tri-*n*-butyl-[3-(trimethoxysilyl)propyl]phosphonium chloride (0.9 ml) and 25 % aqueous ammonia was stirred with a magnetic stirring bar at room temperature for 2 hr. The glass plate (18 x 18 mm^2 pieces) was dipped into this methanol solution at room temperature and left for 5 min. This was lifted from the solution at a constant rate of 0.5 mm/min, and subjected to the treatment for 1 day at room temperature, and finally dried in vacuo for 1 day at room temperature. After drying, the contact angles of water and dodecane for this glass plate were measured. The contact angle values for dodecane and water were measured with a Drop Master 300 (Kyowa Interface Science Co.) by depositing a drop of dodecane or water (2 μl) on the modified glass (18 x 18 mm^2 pieces) surface, which was left in the box (55 mm x 98 mm x 26 mm) and equipped with a temperature controller after the pre-incubation of the modified glass left in this box at each temperature (20 ~ 50 ^oC) for 1 hr.

2.3. Results and discussion

Sol-gel reaction of fluoroalkyl end-capped vinyltrimethoxysilane oligomer in the presence of tri-*n*-butyl[3-(trimethoxysilyl)propyl]phosphonium chloride [TBSiPCl] was found to proceed smoothly under alkaline conditions to afford the corresponding

oligomer/TBSiPCl/SiO_2 composites in 53 ~ 58 % isolated yields. These results were shown in Scheme 2-1.

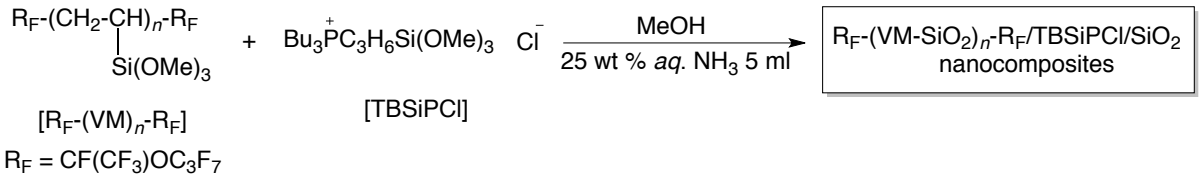

NC (Nanocomposite)	R_F-(VM)$_n$-R_F (g)	TBSiPCl (ml)	Product Yields (%)*
1	0.10	0.9	53
2	0.15	0.9	54
3	0.20	0.9	58

Scheme 2-1

These obtained composites have a good dispersibility in not only water but also organic media such as methanol, ethanol, and tetrahydrofuran. Thus, SEM (scanning electron microscopy) photographs of R_F-(VM)$_n$-R_F/TBSiPCl/SiO_2 nanocomposites have been measured, and the results were shown in Fig. 2-1. SEM images showed the formation of fine fluorinated composite nanoparticles with a mean diameter of 45 nm (Fig. 2-1).

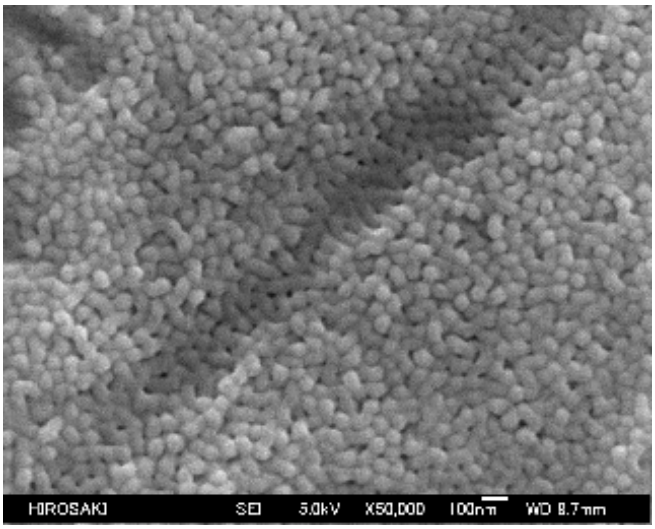

Fig. 2-1 SEM (scanning electron microscopy) images of R_F-$(VM)_n$-R_F/TBSiPCl/SiO_2 nanocomposites (NC 2 in Scheme 2-1) in methanol solutions

It is in particular interest to apply these fluorinated nanocomposites to the surface modification of glass. In fact, the R_F-$(VM)_n$-R_F/TBSiPCl/SiO_2 nanocomposites were applied to the surface modification of glass, and the contact angles of dodecane and water on the modified glasses were measured. The contact angles of dodecane and water, of whose results are the identical values derived from three time repeat experiments, on the modified glass surfaces treated with R_F-$(VM)_n$-R_F/TBSiPCl/SiO_2 nanocomposites were shown in Table 2-1 and Figs. 2-2 and 2-3.

Table 2-1 Contact angles of dodecane and water on the modified glass treated with R_F-$(VM)_n$-R_F/TBSiPCl/SiO_2 nanocomposites (NC 1 ~ 3 in Scheme 2-1) at 20 ℃.

NC	Dodecane	Water (Degree)						
		0 min	5 min	10 min	15 min	20 min	25 min	30 min
1	58	6	0	0	0	0	0	0
2	62	10	0	0	0	0	0	0
3	48	15	0	0	0	0	0	0

Dodecane contact angle: 58°

Fig. 2-2 Charged coupled device camera image of the dodecane droplet on the modified glass surface treated with R_F-$(VM)_n$-R_F/TBSiPCl/SiO_2 nanocomposites at 20 ℃ (used nanocomposites: NC 1 in Scheme 2-1).

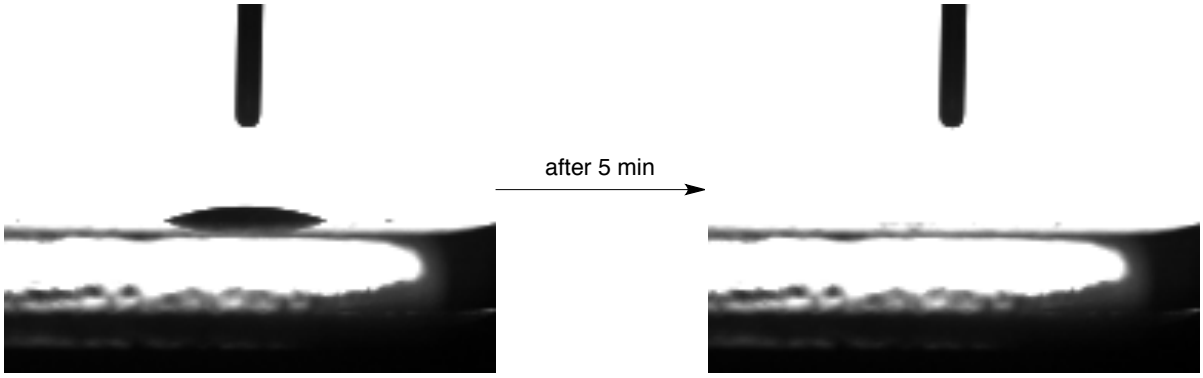

Fig. 2-3 Charged coupled device camera image of the water droplets on the modified glass surface treated with R_F-$(VM)_n$-R_F/TBSiPCl/SiO_2 nanocomposites (used nanocomposites: NC 1 in Scheme 2-1) at 20 ℃ (initial water contact angle (A) and water contact angle after 5 min (B)).

As shown in Table 2-1 and Fig. 2-2, the contact angle of dodecane on each modified glass surface showed significantly large values: 48 ~ 62 degrees, which indicates a high oleophobicity imparted by fluoroalkyl segments in nanocomposites on the modified glass surface, compared to that (0 degree) of the non-treated glass. On the other hand, quite interestingly, the oleophobic (by fluoroalkyl groups in nanocomposites) to superhydrophilic (water contact angle: 0^o) switching behavior can be easily observed on the modified surface when the surface environment is changed from air to water, and it takes only 5 min to replace the fluoroalkyl groups by ionic liquid segments when the surface is in contact with liquid water (see Table 2-1 and Fig. 2-3).

R_F-$(VM\text{-}SiO_2)_n$-R_F oligomeric nanoparticles, which were prepared by the sol-gel reactions of R_F-$(VM)_n$-R_F oligomer under alkaline conditions, have been already applied as

surface modifiers to exhibit a superhydrophobic characteristic (water contact angle: 180°).[30] In this case, fluoroalkyl groups in R_F-(VM-SiO_2)$_n$-R_F oligomeric nanoparticles are located at a fractal surface to exhibit a superhydrophobic property.[30] However, as shown in Fig. 2-4, the relatively smooth surface was observed on modified glass (NC 1 as shown in Table 2-1) by DFM (Dynamic Force Mode) measurements. This relatively smooth surface could afford oleophobic and hydrophilic characteristics in Table 2-1.

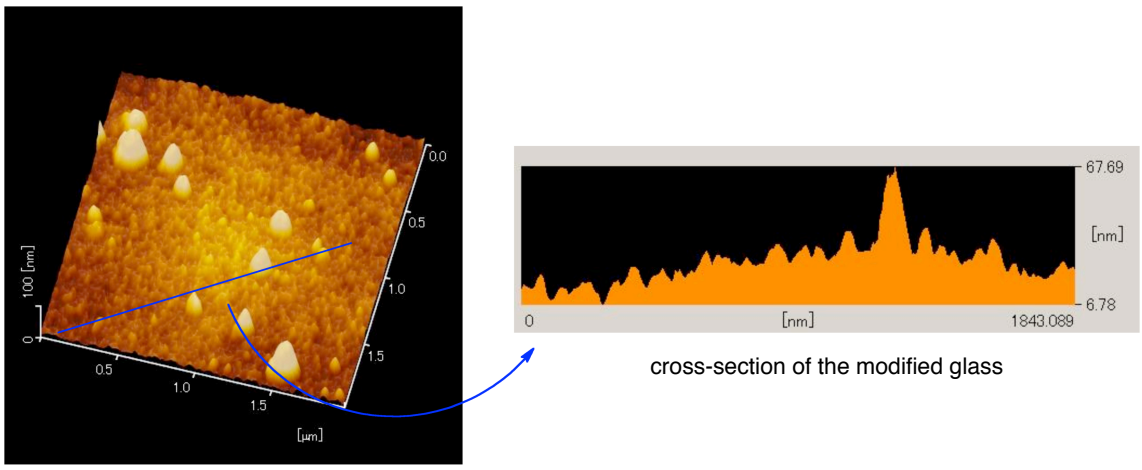

Fig. 2-4 DFM (dynamic force microscopy) images of the modified glass surface treated with R_F-(VM)$_n$-R_F/TBSiPCl/SiO_2 nanocomposites (NC 1 in Table 2-1).

It is well-known that traditionally inorganic and organic materials such as ceramics, polystyrene, and poly(tetrafluoroethylene) can exhibit hydrophilic-oleophilic, hydrophobic-oleophilic, and hydrophobic-oleophobic characteristics, respectively.[26] However, we have in general some difficulties to develop the materials possessing both

hydrophilic and oleophobic characteristics.[26] On the other hand, these present fluorinated nanocomposites consist of not only strong oleophobic segments (fluoroalkyl groups) but also strong hydrophilic segments (ionic liquid) in their silica matrices. This molecular design in these present nanocomposites could enable the modified glass surface to afford the novel oleophobic to superhydrophilic switching behavior.

It is well known that block copolymers such as poly(*N*-isopropylacrylamide)-*block*-poly(ethylene oxide) exhibit thermosensitive micellization because of the hydrophobic character of the poly(*N*-isopropylacrylamide) block above its LCST (Lower Critical Solution Temperature) combined with the hydrophilic property of the poly(ethylene oxide) block in aqueous systems.[31] Similarly, fluoroalkyl end-capped 2-acrylamide-2-methylpropane-sulfonic acid cooligomeric nanoparticles containing adamantyl units can exhibit the LCSTs around 50 ^{o}C in *t*-butyl alcohol, indicating that this LCST behavior would be mainly due to the oleophilic-oleophobic balance corresponding to the oleophilic character from adamantyl segments and the oleophobic character from fluoroalkyl groups.[32] Therefore, it would become possible to observe the decrease of the contact angles for dodecane at the modified glass surface by raising the temperature, due to the oleophilic-oleophilic interaction between dodecane and ionic liquid segments in nanocomposites.

In fact, the contact angle values for dodecane have been measured on the modified glass

surface treated with fluorinated nanocomposites at 20, 40, and 50 °C. These results are shown in Table 2-2.

Table 2-2 Relationship between the temperatures of modified glass surface and dodecane contact angles on the modified glass surface treated with R_F-$(VM)_n$-R_F/TBSiPCl/SiO_2 nanocomposites (used nanocomposites: NC 3 in Scheme 2-1), and the decrease rates of dodecane contact angle values*.

Temp (℃)	Dodecane (Degree)							k x 10^2
	0 min	5 min	10 min	15 min	20 min	25 min	30 min	(min^{-1})
20	48	—	47	—	46	46**	46**	0.21
40	43	—	41	—	40	39	38	0.41
50	42	41	—	—	38	—	36	0.51

*) Decrease rates: $\ln(CA_0/CA_{t=t}) = kt$; CA = dodecane contact angle values

**) These data were not included in the decrease rates

A strong time dependence of contact angles values for dodecane was observed in the fluorinated nanocomposites at 20 ~ 50 °C over 30 min. The first-order rate constants (k) were determined for the decrease of contact angle values for dodecane at these temperatures, although the physical meaning for the rate constant: k would not be clarified at the present time. The results were also shown in Table 2-2.

The decrease ratio was found to follow good first-order equation to increase from k = 0.21 x 10^{-2} to 0.51 x 10^{-2} (min^{-1}) with the increase of the temperatures from 20 to 50 °C. This finding suggests that the oleophilic – oleophilic interaction between the oleophilic moieties in nanocomposites and dodecane should cause the smooth flip-flop motion between the

fluoroalkyl groups and oleophilic moieties in nanocomposites under such conditions on the modified glass surface to exhibit the LCST-like characteristic toward air atmosphere. Especially, oleophilic–oleophilic interaction between the ionic liquid segments in nanocomposites and dodecane should become stronger toward air atmosphere on the surface, compared to the oleophobic interaction between the fluoroalkyl groups and dodecane under higher temperature conditions.

2.4. Conclusion

In summary, the novel fluoroalkyl end-capped vinyltrimethoxysilane oligomer – tri-*n*-butyl[3-(trimethoxysilyl)propyl]phosphonium chloride [TBSiPCl]/silica nanocomposites were prepared by the sol-gel reaction of the corresponding oligomer in the presence of TBSiPCl under alkaline conditions. The modified glass surface treated with these fluorinated nanocomposites can exhibit a strong oleophobicity imparted by fluorocarbon. Interestingly, this modified glass surface can exhibit a superhydrophilicity related to the presence of TBSiPCl in nanocomposites when the environment is changed from air to water on the surface. Furthermore, the higher adhesion ability was obtained between the glass surface and these fluorinated nanocomposites, because the almost same contact angle values

for dodecane and water on the modified glass surface were observed even after washing with water 3 times due to the presence of trimethoxysilyl groups in the nanocomposites. Thus, these fluorinated nanocomposites have high potential for the applications to the surface modification in a wide variety of fields.

References

1) T. Welton, *Chem. Rev*., **99**, 2071 (1999).

2) J. Dupont and J. Spencer, *Angew. Chem. Int. Ed.*, **43**, 5296 (2004).

3) T. Welton, *Coord. Chem. Rev*., **248**, 2459 (2004).

4) P. Wassercheid and W. Keim, *Angew. Chem. Int. Ed.*, **39**, 3772 (2000).

5) J. L. Anderson, D. W. Armstrong, and G. T. Wie, *Anal. Chem*., **78**, 2892 (2006).

6) K. Shimojo, K. Nakashima, N. Kamiya, and M. Goto, *Biomacromolecules*, **7**, 2 (2006).

7) K. Shimojo, N. Kamiya, F. Tani, H. Naganawa, Y. Naruta, and M. Goto, *Anal. Chem.,* **78**, 7735 (2006).

8) C. D.-Hong, C. X.-Wei, S. Yang, and W. J.-Hua, *Chin. J. Anal. Chem*., **36**, 1187 (2008).

9) Y. Okada and H. Sawada, *Colloid Polym. Sci*., **287**, 1359 (2009).

10) R. Hagiwara and Y. Ito, *J. Fluorine Chem*., **105**, 221 (2000).

11) J. G. Huddleston, A. E. Visser, W. M. Reichert, H. D. Willauer, G. A. Broker, and R. D. Rogers, *Green Chem.*, **3**, 156 (2001).

12) Z. Ma, J. Yu, and S. Dai, *Adv. Mater.*, **22**, 261 (2010).

13) X. He, W. Yang, and X. Pei, *Macromolecules*, **41**, 4615 (2008).

14) T. Cremer, M. Killian, J. M. Gottfried, N. Paape, P. Wasserscheid, F. Maier, and H.-P. Steinruck, *Chem. Phys. Chem*., **9**, 2185 (2008).

15) X. Hu, J. Huang, W. Zhang, M. Li, C. Tao, and G. Li, *Adv. Mater*., **20**, 4074 (2008).

16) M. Zhu, J. Yan, Y. Mo, and M. Bai, *Tribol. Lett.*, **29**, 177 (2008).

17) X. Lu, J. Zhou, Y. Zhao, Y. Qiu, and J. Li, *Chem. Mater*., **20**, 3420 (2008).

18) M. Dobbelin, R. T.-Zaera, R. Marcilla, J. Iturri, S. Moya, J. A. Pomposo, and D. Mecerreyes, *Adv. Funct. Mater*., **19**, 3326 (2009).

19) U. Bardi, S. P. Chenakin, S. Caporali, A. Lavacchi, I. Perissi, and A. Tolstogouzov, *Surface Interface Analysis*, **38**, 1768 (2006).

20) T. Cai, H. Zhang, Q. Guo, H. Shao, and X. Hu, *J. Appl. Polym. Sci.*, **115**, 1047 (2010).

21) H. Sawada, *Chem. Rev*., **96**, 1779 (1996).

22) H. Sawada, *J. Fluorine Chem*., **105**, 219 (2000).

23) H. Sawada, *Prog. Polym. Sci*., **32**, 509 (2007).

24) H. Sawada, *Polym. J.,* **39**, 637 (2007).

25) H. Sawada, K. Yanagida, Y. Inaba, M. Sugiya, T. Kawase, and T. Tomita, *Eur. Polym. J.* **37**, 1433 (2001).

26) H. Kakehi, M. Miura, N. Isu, and H. Sawada, *Polym. J.*, **40,** 1081 (2008).

27) H. Sawada, D. Tamada, T. Kawase, Y. Hayakawa, and M. Baba, *Macromolecules*, **30**, 6706 (1997).

28) H. Sawada, Y. Ikematsu, T. Kawase, and Y. Hayakawa, *Langmuir*, **12**, 3529 (1996).

29) H. Sawada and M. Nakayama, *J. Chem. Soc., Chem. Commun*., 677 (1991).

30) H. Sawada, T. Suzuki, H. Takashima, and K. Takishita, *Colloid Polym. Sci*., **286**, 1569 (2008).

31) M. D. C.Topp, P. J. Dijksta, H. Talsma, and J. Feijin, *Macromolecules*, **30**, 8518 (1997).

32) M. Mugisawa, K. Ohnishi, and H. Sawada, *Langmuir*, **23**, 5848 (2007).

CHAPTER 3

Preparation and Applications of Fluoroalkyl End-capped Vinyltrimethoxysilane Oligomeric Nanoparticle Ionogels

3.1. Introduction

Ionic liquids consist entirely of ions and have hitherto attracted continuous interest due to their remarkable physico-chemical properties, including high thermal and chemical stability, non-flammability, negligible vapor pressure, and electrical and ionic conductivities.[1 ~ 3] Ionic liquids have been also developed as components in functional hybrid materials that are termed ionogels.[4] Ionogels are in general prepared by hybridizing ionic liquids with another components such as organic gelator, polymer, carbon nanotubes and inorganic metal oxide nanoparticles.[5 ~ 8] In these ionogels, silica-based ionogels are easily obtained by the confinement of ionic liquids in a silica network, and such networks can be achieved through the gelation of colloidal silica particles in the ionic liquids.[9 ~ 12] The resulting solid-like materials are interesting candidates for solid electrolytes in next-generation electrochemical devices such as solar cells and fuel cells.[13 ~ 16] Comprehensive studies have been hitherto focused on the preparation and properties of fluoroalkyl end-capped vinyltrimethoxysilane oligomeric silica nanoparticles through the sol-gel reaction of the corresponding oligomer [R_F-(CH_2-$CHSi(OMe)_3)_n$-R_F: the mixture of dimer and trimer; R_F = $CF(CF_3)OC_3F_7$: R_F-$(VM)_n$-R_F] under alkaline conditions.[17] Fluoroalkyl end-capped vinyltrimethoxysilane oligomeric silica nanoparticles thus obtained can exhibit the completely superhydrophobic

characteristic (water contact angle value: 180^{o}) with good oleophobic property on the modified glass surface.[18] Therefore, it is in particular interest to explore new fluoroalkyl end-capped vinyltrimethoxysilane oligomeric silica nanoparticle-based ionogels imparted by the surface active characteristic related to the longer fluoroalkyl groups, from the developmental viewpoints of novel fluorinated functional hybrid materials; however, such studies have been hitherto very limited except for the previous report for the gelation of an ionic liquid (*N*-methylpyrazolium tetrafluoroborate) by fluoroalkyl end-capped 2-acrylamido-2-methyl-propanesulfonic acid oligomer.[19] Here, this Chapter shows that the fluoroalkyl end-capped vinyltrimehoxysilane oligomeric silica nanoparticles, which are prepared by the sol-gel reaction of the corresponding oligomer under alkaline conditions, can provide the corresponding fluoroalkyl end-capped oligomeric silica ionogels through the interactions with a variety of ionic liquids under ultrasonic irradiation. Interestingly, these obtained fluoroalkylated ionogels can afford a similar ionic conductivity to that of the parent ionic liquids, and are applicable to the surface modification of traditional organic polymers such as poly(methyl methacrylate) [PMMA] to exhibit not only the surface active characteristic imparted by longer fluoroalkyl groups in the ionogels but also the good surface ionic conductivity relevant to the ionic liquids. More interestingly, the switching behavior from oleophobic to superhydrophilic characteristics was observed under the flip-flop motion

between the fluoroalkyl groups and the cationic moieties when the environment on the reverse side is changed from oil to water. These results will be described in this Chapter.

3.2. Experimental

3.2.1. Measurements

Dynamic light scattering (DLS) measurements were measured by using Otsuka Electronics DLS-7000 HL (Tokyo, Japan). Contact angles were measured using a Kyowa Interface Science Drop Master 300 (Saitama, Japan). Field emission scanning electron micrographs (FE-SEM) were obtained by using JEOL JSM-7000F (Tokyo, Japan).

3.2.2. Materials

Tributylallylphosphonium bis(trifluoromethanesulfonyl)imide [TBAP-BTFSI], triethyl-dodecylammonium bis(trifluoromethanesulfonyl)imide [TEDA-BTFSI], tributylmethyl-phosphonium dimethylphosphate [TBMP-DMP], and tributyl[3-(trimethoxysilyl)propyl]-phosphonium chloride [TBTMSiP-Cl] were received from Nippon Chemical Industrial Co.,

Ltd., Tokyo, Japan. 1-Ethyl-3-methylimidazolium bis(trifluoromethanesulfonyl)imide [EMI-BTFSI] was purchased from Kanto Chemical Co., Ltd., Tokyo, Japan. *N*-Methylpyrazolium tetrafluoroborate [NMP-BF4] and 1-buthyl-3-metylimidazolium hexa-fluorophosphate [BMI-PF6] were received from Stella Chemifa Corp. (Osaka, Japan) and Merck KGaA (Darmstadt, Germany), respectively. 1-Ethyl-3-methylimidazolium hydrogen sulfate [EMI-HSO4] and tetraethoxysilane were purchased from Tokyo Chemical Industrial Co., Ltd. (Tokyo, Japan). Silica nanoparticles (Methanol Silica-sol^{TR}) were received from Nissan Chemical Industrials Ltd., Tokyo, Japan. Aqueous ammonia was purchased from Wako Pure Chemical Industries, Ltd. (Osaka, Japan). Fluoroalkyl end-capped vinyltrimethoxysilane oligomer [R_F-(CH_2-$CHSi(OMe)_3)_n$-R_F: the mixture of dimer and trimer; R_F = $CF(CF_3)OC_3F_7$] was prepared by reaction of fluoroalkanoyl peroxide with the corresponding monomer according to the previously reported method.[20)]

3.2.3. Preparation of fluoroalkyl end-capped vinyltrimethoxysilane oligomeric silica nanoparticles [R_F-(VM-$SiO_2)_n$-R_F]

A typical procedure for the preparation of R_F-(VM-$SiO_2)_n$-R_F nanoparticles is as follows: To methanol solution (20 ml) containing fluoroalkyl end-capped vinyltrimethoxy-

silane oligomer [1.00 g; R_F-[$CH_2CHSi(OMe)_3$]$_n$-R_F: R_F = $CF(CF_3)OC_3F_7$; Mn = 730] was added 25 % aqueous ammonia solution (5 ml). The mixture was stirred with a magnetic stirring bar at room temperature for 5 h. After the solvent was evaporated off, methanol was added to the obtained crude products. The methanol suspension was stirred with magnetic stirring bar at room temperature for 1 day, and then was centrifuged for 30 min. The expected fluorinated oligomeric silica particles were easily separated from the methanol solution, and then was washed with methanol in several times. After centrifugal separation of this solution, the obtained product was dried in vacuo at 50 °C for 1 day to produce the purified white colored powders (0.78 g).

3.2.4. Preparation of fluoroalkyl end-capped vinyltrimethoxysilane oligomeric silica nanoparticles [R_F-(VM-SiO_2)$_n$-R_F/SiO_2] by the use of tetraethoxysilane and silica nanoparticles

A typical procedure for the preparation of R_F-(VM-SiO_2)$_n$-R_F/SiO_2 nanoparticles is as follows: To methanol solution (20 ml) containing fluoroalkyl end-capped vinyltrimethoxysilane oligomer [1.00 g; R_F-[$CH_2CHSi(OMe)_3$]$_n$-R_F: R_F = $CF(CF_3)OC_3F_7$; Mn = 730], 30 wt % silica-nanoparticle methanol solution [3.33 g; average particle size: 11 nm

(Methanol Silica-sol^{TR}), and tetraethoxysilane (0.50 ml) was added 25 % aqueous ammonia solution (5 ml). The mixture was stirred with a magnetic stirring bar at room temperature for 5 h. After the solvent was evaporated off, methanol was added to the obtained crude products. The methanol suspension was stirred with magnetic stirring bar at room temperature for 1 day, and then was centrifuged for 30 min. The expected fluorinated oligomeric silica particles were easily separated from the methanol solution, and then was washed with methanol in several times. After centrifugal separation of this solution, the obtained product was dried in vacuo at 50 °C for 1 day to produce the purified white colored powders (1.60 g).

3.2.5. Gelation of ionic liquids by R_F-(VM-SiO_2)$_n$-R_F nanoparticles [or R_F-(VM-SiO_2)$_n$-R_F/SiO_2 nanoparticles]

R_F-(VM-SiO_2)$_n$-R_F nanoparticles (25 mg) [or R_F-(VM-SiO_2)$_n$-R_F/SiO_2 nanoparticles (256 mg)] was added to tri-*n*-butyl[3(trimethoxysilyl)propyl]phosphonium chloride (475 mg). The resulting mixture was treated under ultrasonic conditions for 3 day at 50^{o}C to afford the R_F-(VM-SiO_2)$_n$-R_F nanoparticles-based ionogels (or R_F-(VM-SiO_2)$_n$-R_F/SiO_2 nanoparticles-based ionogels).

3.2.6. Surface modification of poly(methyl methacrylate) treated with the R_F-(VM-SiO_2)$_n$-R_F nanoparticles-based ionogels

The modified PMMA film was prepared by casting the mixed solutions of 1,2-dichloroethane and methanol (v/v) 4/1; 25 ml) containing PMMA (990 mg) and the R_F-(VM-SiO_2)$_n$-R_F nanoparticles–based ionogels (10 mg) on a glass plate. The solvent was evaporated at room temperature and the film formed peeled off and dried at 50 °C for 24 h under vacuum to afford the modified PMMA film. The contact angles of dodecane and water on the surface and the reverse sides of this film were measured at room temperature from goniometer-type contact angle measurements.

3.2.7. Ionic conductivity measurements

The ionic conductivity of the fluoroalkylated ionogels was measured by using Agilent Technologies 34401A (Keysight Technologies, Tokyo). The analysis was conducted in the temperature range from 25 to 125 ^{o}C. The surface ionic conductivities of the modified PMMA film treated with the fluoroalkylated ionogels were measured by using AGILENT 4339B (High Resistance Meter) and Agilent 160008B (Resistivity Cell) (Keysight

Technologies, Tokyo). Before measurements were taken, two stainless steel plate electrodes were contacted onto the modified films.

3.3. Results and discussion

Fluoroalkyl end-capped vinyltrimethoxysilane oligomeric silica nanoparticles [R_F-(VM-SiO_2)$_n$-R_F] were prepared by the sol-gel reaction of the corresponding oligomer under alkaline conditions according to the previously reported method.[18] In addition, fluoroalkyl end-capped vinyltrimethoxysilane oligomeric silica nanoparticles [R_F-(VM-SiO_2)$_n$-R_F/SiO_2] were prepared by the sol-gel reaction of the corresponding oligomer in the presence of tetraethoxysilane (TEOS) and silica nanoparticles under alkaline conditions. These results are shown in Scheme 3-1.

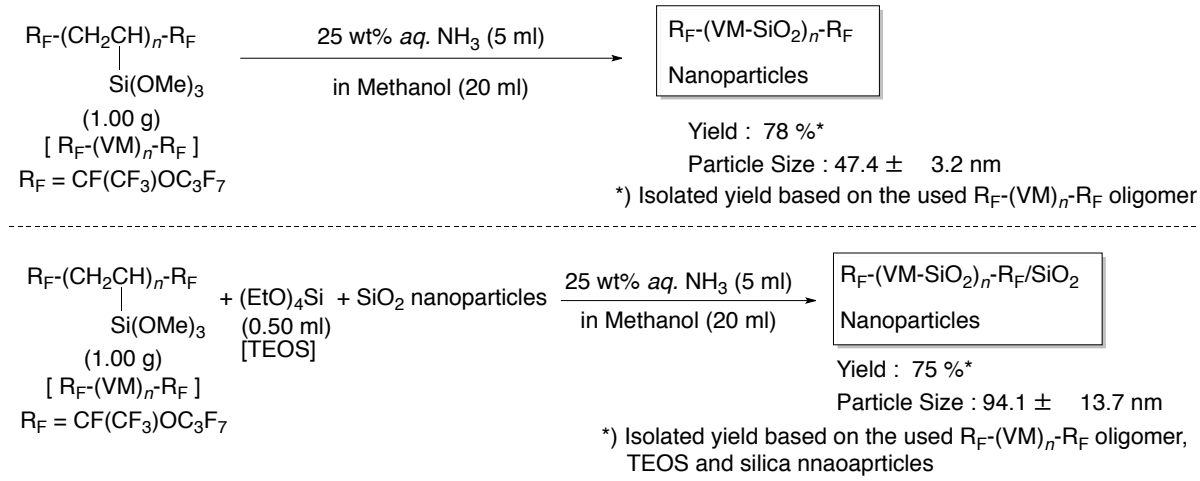

Scheme 3-1 Preparation of R_F-(VM-SiO_2)$_n$-R_F oligomeric nanoparticles and R_F-(VM-SiO_2)$_n$-R_F/SiO_2 oligomeric nanoparticles

Each obtained white-colored powder was found to exhibit an extremely poor dispersibility in water; however, these powders afforded good dispersibility and stability for the traditional organic media such as methanol, ethanol, 2-propanol, tetrahydrofuran, 1,2-dichloroethane, *N,N*-dimethylformamide, dimethyl sulfoxide, and fluorinated aliphatic solvents [1 : 1 mixed solvents (AK-225^{TR}) of 1, 1-dichloro-2, 2, 3, 3, 3-pentafluoropropane and 1, 3-dichloro-1, 2, 2, 3, 3-pentafluoropropane]. Thus, the size of these particles have been measured in methanol by dynamic light scattering (DLS) measurements at 25 °C. Each size of these particles is nanometer size-controlled fine particles: 47.4 ± 3.2 ~ 94.1 ± 13.7 nm (number-average diameter) as shown in Scheme 3-1. A higher average particle size was observed in the R_F-(VM-SiO_2)$_n$-R_F/SiO_2 particles, indicating that the sol-gel reaction with TEOS and silica nanoparticles (average particles size: 11 nm) should proceed smoothly

to give the core-corona type nanoparticles, which consist of silica nanoparticle as the cores units including the siloxane network derived from the sol-gel reaction of tetraethoxysilane as shell units and the fluoroalkyl segments as the corona units. Such sol-gel reaction should afford the higher average particle size, compared with that of R_F-$(VM)_n$-R_F oligomer with no use of both silica nanoparticles and tetraethoxysilane.

The field emission scanning electron micrographs (FE-SEM) of R_F-$(VM\text{-}SiO_2)_n$-R_F nanoparticles and R_F-$(VM\text{-}SiO_2)_n$-R_F/SiO_2 nanoparticles illustrated in Scheme 3-1 have been measured, and the results are shown in Fig. 3-1.

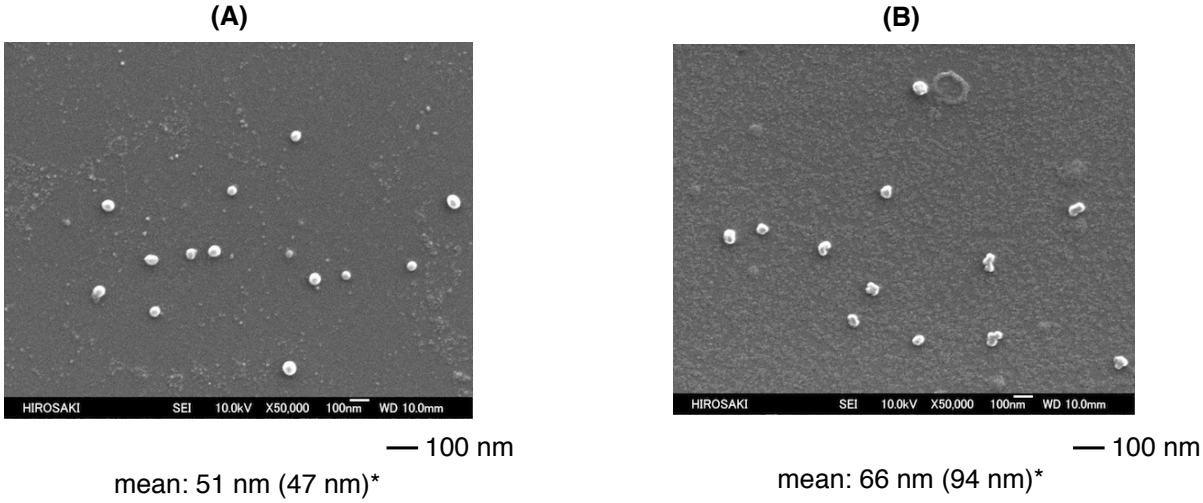

Fig. 3-1 FE-SEM image of methanol solutions of R_F-$(VM\text{-}SiO_2)_n$-R_F nanoparticles **(A)** and R_F-$(VM\text{-}SiO_2)_n$-R_F/SiO_2 nanoparticles **(B)**.

*) Average particle size was determined by DLS measurements.

Fig. 3-1 shows that the uniform fine R_F-$(VM\text{-}SiO_2)_n$-R_F nanoparticles and R_F-$(VM\text{-}SiO_2)_n$-R_F/SiO_2 nanoparticles can be prepared through the sol-gel reaction illustrated

in Scheme 3-1. Electron micrographs of these particles also show the formation of fluorinated oligomeric silica fine particles with mean diameters of 51 and 66 nm, respectively, and the similar size values as those (47 and 94 nm) of DLS were obtained in FE-SEM measurements.

These R_F-(VM-SiO_2)$_n$-R_F nanoparticles and R_F-(VM-SiO_2)$_n$-R_F/SiO_2 nanoparticles can provide a good dispersibility and stability toward the traditional organic solvents except for water. Thus, the dispersibility of these fluorinated nanoparticles was studied in a variety of ionic liquids. The used ionic liquids are shown in Fig. 3-2.

Structure	Abbreviation	Structure	Abbreviation
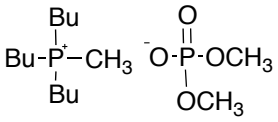	[TBMP-DMP]	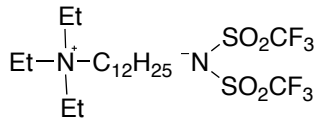	[TEDA-BTFSI]
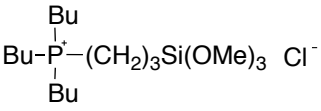	[TBTMSiP-Cl]	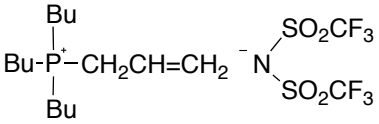	[TBAP-BTFSI]
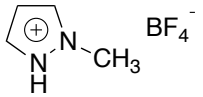	[NMP-BF4]	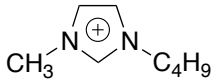	[BMI-PF6]
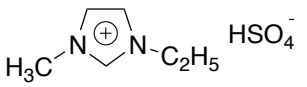	[EMI-HSO4]	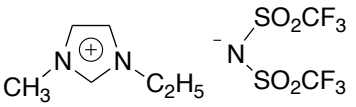	[EMI-BTFSI]

Fig. 3-2 Molecular structures and abbreviations of ionic liquids used

As shown in Fig. 3-3, the R_F-(VM-SiO_2)$_n$-R_F/SiO_2 nanoparticles and the R_F-(VM-SiO_2)$_n$-R_F nanoparticles were found to cause a gelation in TBMP-DMP under ultrasonic conditions.

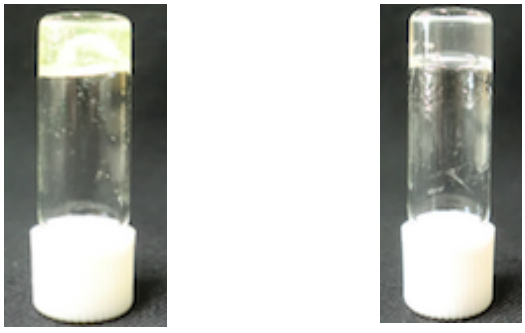

(a) **(b)**

Fig. 3-3 Photograph of R_F-(VM-SiO_2)$_n$-R_F/SiO_2/TBMP-DMP ionogels: **(a)** and R_F-(VM-SiO_2)$_n$-R_F/TBMP-DMP ionogels: **(b)**

The gelling ability of the R_F-(VM-SiO_2)$_n$-R_F oligomeric nanoparticles toward the ionic liquids is in general superior to that of the R_F-(VM-SiO_2)$_n$-R_F/SiO_2 nanoparticles; however, this nanoparticle was not a useful gelator for some ionic liquids such as 1-butyl-3-methylimidazolium hexafluorophosphate [BMI-PF6], 1-methylpyrazolium tetrafluoroborate [NMP-BF4], 1-ethyl-3-methylimidazolium bis(trifluoromethanesulfonyl)-imide [EMI-BTFSI] and 1-ethyl-3-methylimidazolium hydrogen sulfate [EMI-HSO4]. This finding suggests that since R_F-(VM-SiO_2)$_n$-R_F/SiO_2 oligomeric nanoparticles are constructed from the core-corona type-nanoparticles, such core-corona structures should

accelerate the gelation of ionic liquids as illustrated in Scheme 3-2.

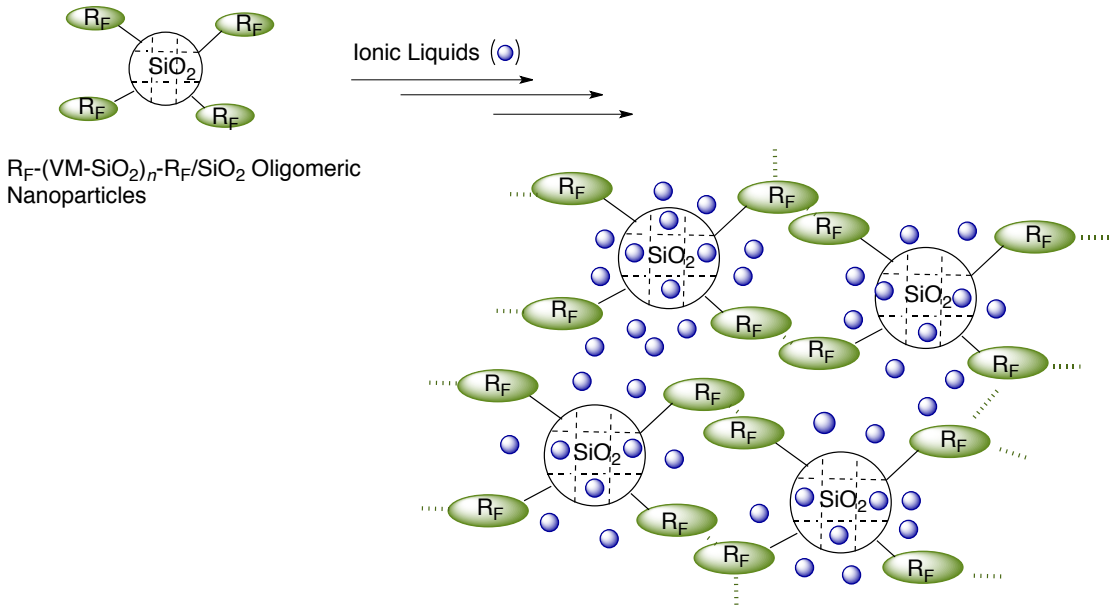

Scheme 3-2 Schematic illustration for the gelation of ionic liquids in the presence of fluoroalkyl end-capped oligomeric silica nanoparticles

To study the gel-formation ability, the minimum concentrations of the R_F-(VM-SiO_2)$_n$-R_F/SiO_2 oligomeric nanoparticles and the R_F-(VM-SiO_2)$_n$-R_F nanoparticles necessary for gelation were measured according to a method reported by Hanabusa et al. [21, 22], and the results on the minimum concentration for gelation (C_{min}) in the ionic liquids at 25 °C were shown in Table 3-1.

Table 3-1 Critical gel concentration: C_{min} (%) and ionic conductivities [σ (mS/cm)] of R_F-(VM-SiO_2)$_n$-R_F/SiO_2 ionogels and R_F-(VM-SiO_2)$_n$-R_F ionogels at 25 °C

Ionic liquid	R_F-(VM-SiO_2)$_n$-R_F/SiO_2 ionogels		R_F-(VM-SiO_2)$_n$-R_F ionogels	
	C_{min} (%)	Ionic conductivities [σ (mS/cm)]	C_{min} (%)	Ionic conductivities [σ (mS/cm)]
TBMP-DMP	40	0.2	10	11
TBTMSiP-Cl	35	6.8	5	17
NMP-BF4	35	686	--*	--**
EMI-HSO4	35	6.4	--*	--**
TEDA-BTFSI	40	7.4	10	6.9
TBAP-BTFSI	40	0.02	5	7.4
BMI-PF6	40	7.4	--*	--**
EMI-BTFSI	40	5.1	--*	--**

*)Gelation was not observed

**) Not determined

C_{min}s of the R_F-(VM-SiO_2)$_n$-R_F/SiO_2 nanoparticles and the R_F-(VM-SiO_2)$_n$-R_F nanoparticles necessary to gel of the ionic liquids are 35 ~ 40 and 5 ~ 10 wt%, respectively. C_{min} values indicate that the gelling ability of the R_F-(VM-SiO_2)$_n$-R_F nanoparticles is superior to those of the R_F-(VM-SiO_2)$_n$-R_F/SiO_2 nanoparticles. This finding suggests that the R_F-(VM-SiO_2)$_n$-R_F nanoparticle networks are likely to interact with the ionic liquids to form the corresponding fluoroalkylated ionogels due to the use of no silica nanoparticles as the core units under the preparative conditions of the expected nanoparticles, different from that of the R_F-(VM-SiO_2)$_n$-R_F/SiO_2 nanoparticles. In fact, the clear network structures can be found in the FE-SEM images of the R_F-(VM-SiO_2)$_n$-R_F/TBTMSiP-Cl ionogels [see Fig. 3-4(a)], although the R_F-(VM-SiO_2)$_n$-R_F/SiO_2/TBTMSiP-Cl ionogels form the fiber-like

assemblies having partly network structures [see Fig. 3-4(b)]. Similar network structures have been already observed in the *N*-isopropylacrylamide polymer ionogels.[23)]

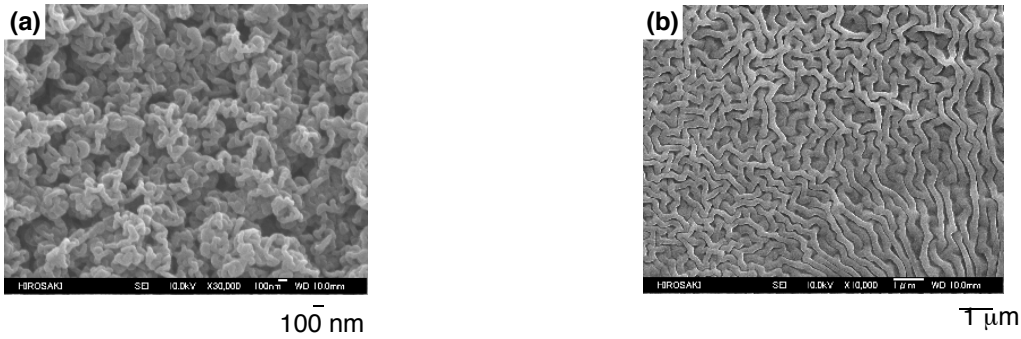

Fig. 3-4 FE-SEM (field emission scanning electron microscopy) images of R_F-(VM-SiO_2)$_n$-R_F/TBTMSiP-Cl ionogels **(a)** and R_F-(VM-SiO_2)$_n$-R_F/SiO_2/TBMP-DMP ionogels (**b)**.

The fluorinated nanoparticle ionogels have been tested for the ionic conductivity, and the results are also shown in Table 3-1. R_F-(VM-SiO_2)$_n$-R_F ionogels and R_F-(VM-SiO_2)$_n$-R_F/SiO_2 ionogels were found to exhibit proton conductivities of $10 \sim 10^{-2}$ mS/cm levels. A higher ionic conductivity was in general observed in the R_F-(VM-SiO_2)$_n$-R_F nanoparticle-ionogels, indicating that their higher gelling ability should enhance the ionic conductivity in the fluorinated oligomeric nanoparticle cores. In these ionogels, an extremely higher ionic conductivity was observed in the R_F-(VM-SiO_2)$_n$-R_F/SiO_2/NMP-BF4 ionogels. This finding is due to the presence of the >N-H proton in NMP-BF4.

To estimate the ionic conductivities of the R_F-(VM-SiO_2)$_n$-R_F ionogels [ionic liquids:

TBTMSiP-Cl, TBAP-BTFSI] possessing a higher gelling ability, their conductivities were measured at various temperatures between 25 and 125 °C. These results are shown in Figs. 3-5 and 3-6, together with those of the corresponding parent ionic liquids, for comparison.

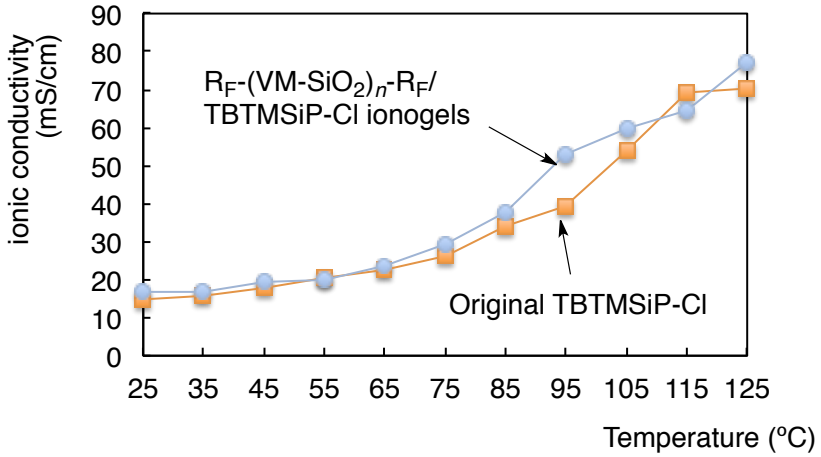

Fig. 3-5 Temperature dependencies of the ionic conductivities of R_F-(VM-SiO_2)$_n$-R_F/TBTMSiP-Cl ionogels and the original TBTMSiP-Cl: Concentration of gelator: 10 wt %

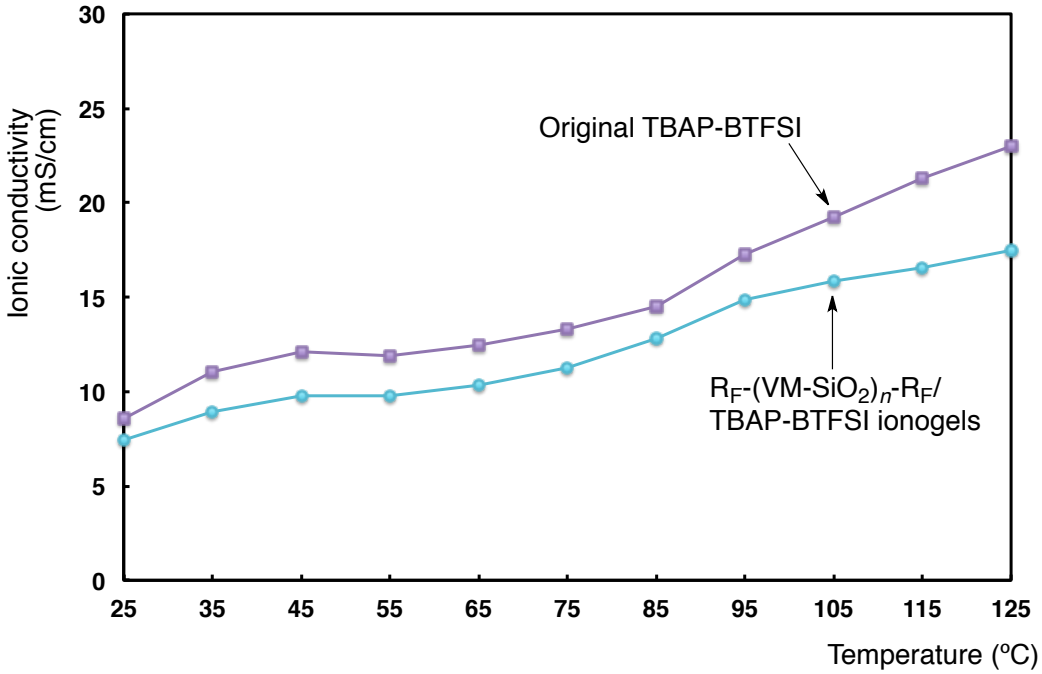

Fig. 3-6 Temperature dependencies of the ionic conductivities of R_F-(VM-SiO_2)$_n$-R_F/TBAP-BTFSI ionogels and the original TBAP-BTFSI: Concentration of gelator: 10 wt %

As shown in Figs. 3-5 and 3-6, the ionic conductivities of the R_F-(VM-SiO_2)$_n$-R_F ionogels were found to increase with the increase of temperatures, and a similar conductivity to that of the original ionic liquids was obtained in each temperature. More interestingly, the ionic conductivities at 125 °C can keep the similar values even after 10 hrs, as well as those of the original ionic liquids (see Figs. 3-7 and 3-8). Therefore, those fluorinated oligomeric silica nanoparticle ionogels are promising candidates for the proton exchange fuel cells.

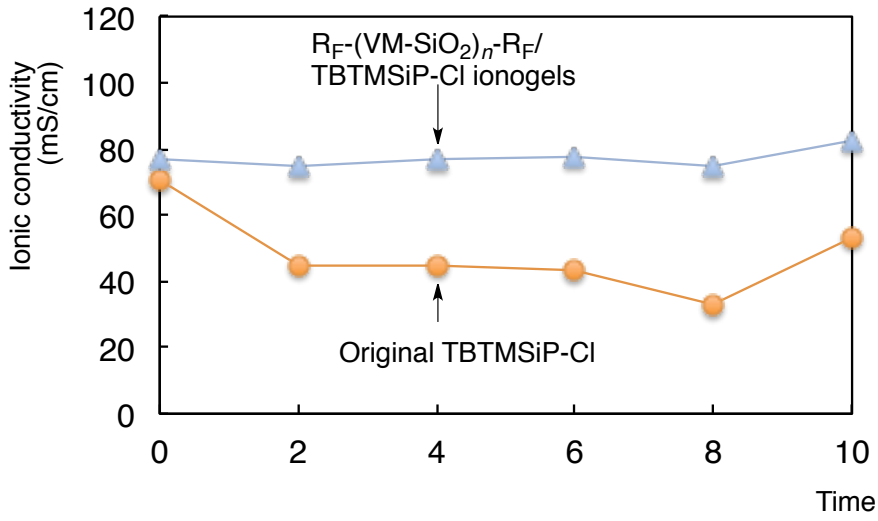

Fig. 3-7 Time dependencies of the ionic conductivities of R_F-(VM-SiO_2)$_n$-R_F/TBTMSP-Cl ionogels and the original TBTMSP-Cl at 125 ºC: Concentration of gelator: 10 wt %

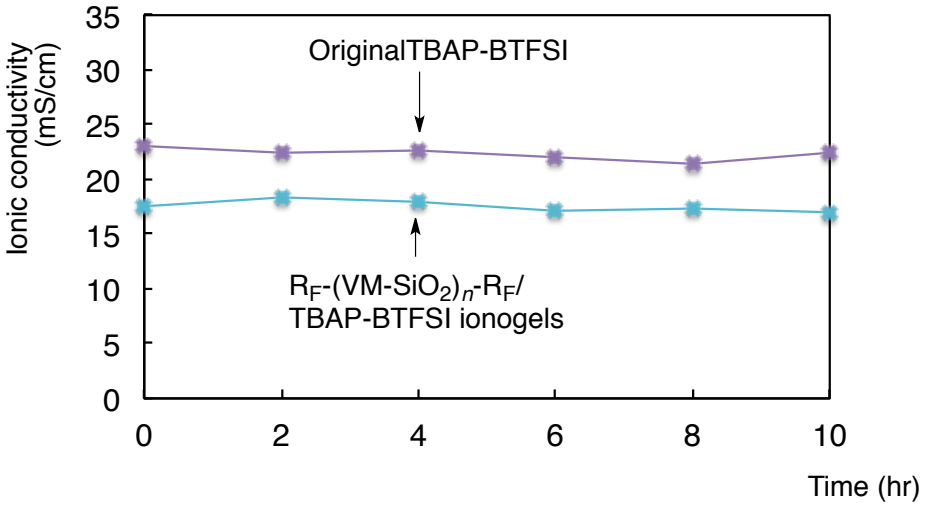

Fig. 3-8 Time dependencies of the ionic conductivities of R_F-(VM-SiO_2)$_n$-R_F/TBAP-BTFSI ionogels and the original TBAP-BTFSI at 125 ºC: Concentration of gelator: 10 wt %

In a variety of partially fluoroalkylated polymers, especially, ABA triblock-type fluoroalkyl end-capped oligomers [R_F-(M)$_n$-R_F; R_F = fluoroalkyl groups; M = radical polymerizable monomers] are attractive functional polymers, because they are very soluble

and can form nanoscale controlled molecular aggregates.[24, 25] These fluorinated molecular aggregates can also interact with a variety of guest molecules such as fullerene and metal nanoparticles as guest molecules to afford the corresponding fluorinated oligomer/guest molecules nanocomposites.[26 ~ 28] Ionic liquids are also smoothly encapsulated into these fluorinated oligomeric aggregate cores to give the fluorinated oligomer/ionic liquids nanocomposites.[29, 30] Ionic liquids have been hitherto applied to the architecture of smart surfaces with their counter anion-responsiveness to exhibit their hydrophilicity and hydrophobicity by simple exchange counter anions.[31, 32] From this point of view, fluorinated oligomer/ionic liquids composites have been already applied to the surface modification of glass to exhibit the superhydrophilicity derived from the hydrophilic cationic segments in ionic liquids through the flip-flop motion between end-capped fluoroalkyl groups and the ionic liquid segments in the composites when the surface environment is changed from air to water.[30] Thus, the R_F-(VM-SiO_2)$_n$-R_F/TBTMSiP-Cl ionogels, which can exhibit not only a higher gelling ability but also a good ionic conductivity, were applied to the surface modification of PMMA, and the dodecane and water contact angle values were measured on the modified PMMA film surfaces. The surface ionic conductivities on the modified PMMA films have been also measured. These results are shown in Fig. 3-9 and Table 3-2.

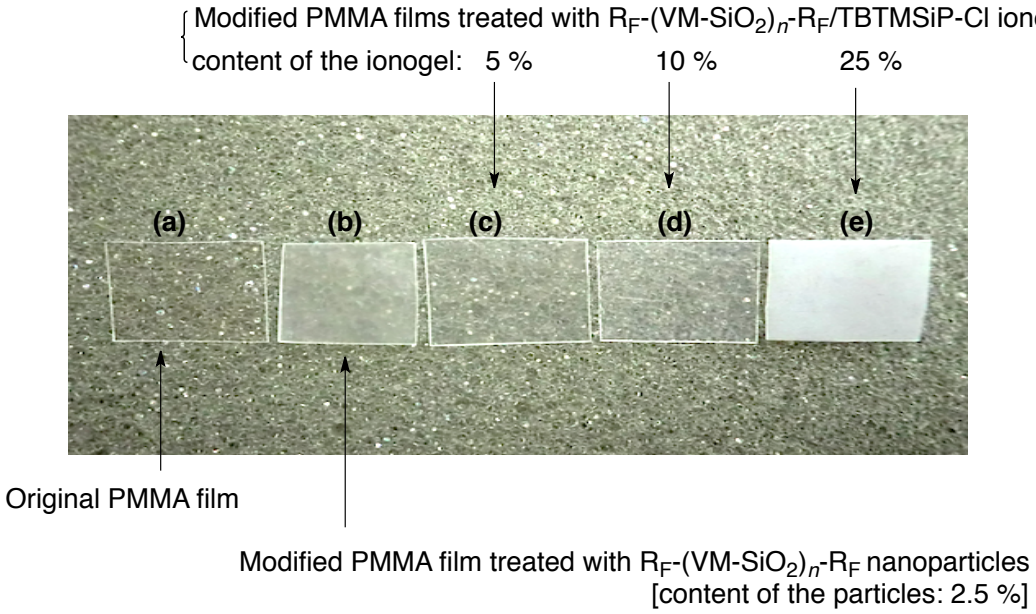

Fig. 3-9 Photograph of modified PMMA films treated with R_F-(VM-SiO_2)$_n$-R_F/TBTMSiP-Cl ionogels

Table 3-2 Dodecane and water contact angle values, and surface ionic conductivities (S/sq.) on the modified PMMA film treated with the R_F-(VM-SiO_2)$_n$-R_F/TBTMSiP-Cl ionogels

Content of the fluorinated ionogel(wt %)*	[Film thickness] (μm)	Contact angle (degree)		Ionic conductivities (S/sq.)	
		Dodecane	Water	Surface side	Reverse side
5	[190]	35 (0)**	102 (61)**	2.2×10^{-12}	1.6×10^{-12}
10	[210]	40 (18)**	103 (30)**	2.1×10^{-12}	3.3×10^{-12}
25	[193]	40 (33)**	97 (52)**	3.2×10^{-12}	9.9×10^{-10}
Original PMMA film	[186]	0 (0)**	74 (73)**	1.3×10^{-12}	1.3×10^{-12}
PMMA film treated with the R_F-(VM-SiO_2)$_n$-R_F oligomeric nanoparticles (Content of the particles: 2.5 wt %)					
	[202]	36 (0)**	95 (70)**	1.3×10^{-12}	1.3×10^{-12}

*) Contents of the fluorinated ionogels based on the used PMMA

**) Reverse side

Fig. 3-9 shows the modified PMMA films treated with the R_F-(VM-SiO_2)$_n$-R_F/TBTMSiP-Cl ionogels. In these modified PMMA films, the contents of

the ionogels: 5 ~ 10 %; see Fig. 3-9-(c) and (d) can give the transparent colorless films, quite similar to that of the parent PMMA film [see Fig. 3-9-(a)]. On the other hand, a higher content (25 %) of the ionogel [see Fig. 3-9-(e)] afforded the white-colored turbid film. The slightly turbid modified film was also prepared by the use of the R_F-(VM-SiO_2)$_n$-R_F oligomeric nanoparticles [see Fig. 3-9-(b)].

Table 3-2 shows that the modified PMMA film surfaces treated with the R_F-(VM-SiO_2)$_n$-R_F/TBTMSiP-Cl ionogels can exhibit a similar oleophobicity with a good hydrophobicity to that of the R_F-(VM-SiO_2)$_n$-R_F oligomeric nanoparticles, compared with that of the original PMMA film. Because, dodecane and water contact angle values on these modified surfaces are 35 ~ 40 degrees and 97 ~ 103 degrees, respectively. However, interestingly, the dodecane contact angle values on the reverse side were found to increase from 0 to 33 degrees with increasing the contents of the fluorinated ionogels from 5 to 25 %. In contrast, the water contact angle values were found to decrease from 61 to 30 or 52 degrees under similar conditions. Hitherto, it is well known that fluoroalkyl end-capped oligomeric nanocomposite-encapsulated fullerene are likely to be arranged regularly on the modified PMMA film surface to exhibit not only a good surface active characteristic imparted by longer fluoroalkyl groups but also the fluorescent property related to the encapsulated fullerene on the surface.[33] However, those fluorinated ionogels can afford an effective

hydrophilic characteristic relevant to the ionic moieties in the ionic liquid, in addition to the oleophobic property (dodecane contact angle value: 18 ~ 33 degrees) imparted by fluorine on the reverse side during the PMMA cast film formation. In particular, a steep dependence of water contact angle on the reverse side can be observed in the case of the content of the ionogels: 25 %, and the water contact angle on the modified PMMA film decreased smoothly from 52 to 0 degrees over 30 min to give the superhydrophilicity on the only reverse side, although such effective decrease of the water contact angles on the surface side cannot be observed as shown in Table 3-3.

Table 3-3 Changes in the water contact angle values on the modified PMMA film surface and reverse sides treated with R_F-(VM-SiO_2)$_n$-R_F/TBTMSiP-Cl ionogels*

	0	5	10	15	20	25	30 (min)
Reverse side (degree)	52	46	39	36	25	18	0
Surface Side (degree)	97	80	72	68	64	62	61

*)Content of the fluorinated ionogels based on the used PMMA: 25 wt%

Similarly, the ionic conductivities on the reverse side was found to increase effectively from 1.6 x 10^{-12} to 9.9 x 10^{-10} S/sq. with the increase of the contents of the fluorinated ionogels from 5 to 25 %.

In this way, it was clarified that those R_F-(VM-SiO_2)$_n$-R_F/TBTMSiP-Cl ionogels are applicable to the surface modification of PMMA to exhibit the good surface active property

imparted by fluoroalkyl groups in the nanoparticles but also the surface ionic conductivities related to the ionic liquids. However, unexpectedly, it was demonstrated that this fluoroalkylated ionogel can afford the oleophobic and superhydrophilic characteristics on the reverse side through the flip-flop motion between the fluoroalkyl groups and the ionic moieties in the ionic liquids as shown in Fig. 3-10.

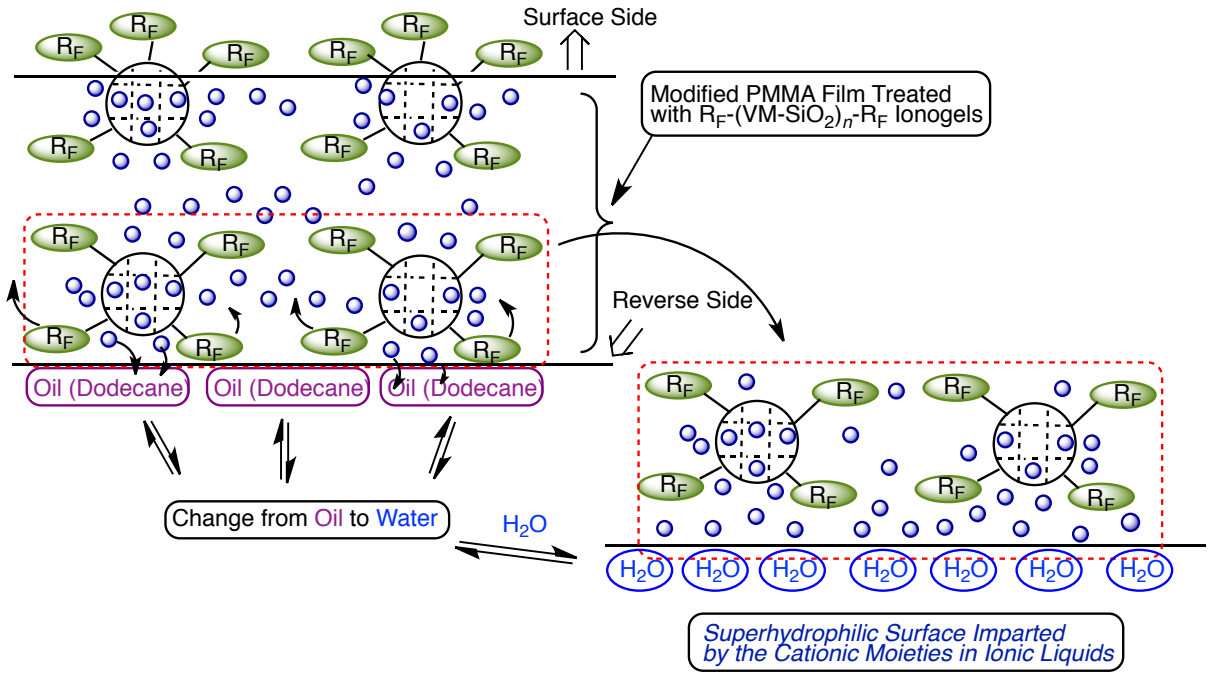

Fig. 3-10 Switching behavior from hydrophobic to superhydrophilic characteristics on the reverse side under the environmental change from oil to water.

This is the first example of the switching behavior between the hydrophobicity and superhydrophilicity with a good oleophobicity on the reverse side.

3.4. Conclusions

Fluoroalkyl end-capped vinyltrimethoxysilane oligomer [R_F-$(VM)_n$-R_F] was applied to the preparation of two-type fluorinated oligomeric silica nanoparticles. One is the fluorinated oligomeric silica nanoparticles [R_F-$(VM\text{-}SiO_2)_n$-R_F], which were prepared by the sol-gel reaction of the corresponding oligomer under alkaline conditions. The other is the fluorinated oligomeric silica nanoparticles [R_F-$(VM\text{-}SiO_2)_n$-R_F/SiO_2], which were prepared by the similar sol-gel reaction with tetraethoxysilane (TEOS) and silica nanoparticles. These obtained fluorinated nanoparticles cannot cause a gelation toward water and the traditional organic media such as methanol, ethanol and tetrahydrofuran; however, these two-type fluorinated oligomeric nanoparticles were effective to cause a gelation toward a variety of ionic liquids such as phosophonium-, ammonium-, pyrazolium-, and imidazolium-type ionic liquids. R_F-$(VM\text{-}SiO_2)_n$-R_F/SiO_2 oligomeric nanoparticles were more effective to cause a gelation, compared with that of the R_F-$(VM\text{-}SiO_2)_n$-R_F oligomeric nanoparticles. In contrast, the gelling ability for these ionic liquids was higher in the R_F-$(VM\text{-}SiO_2)_n$-R_F oligomeric nanoparticles. These two-type fluorinated ionogels were found to afford the good ionic conductivities, quite similar to those of the parent ionic liquids, and to keep the similar ionic conductivities even after 10 hrs at 125 °C. Interestingly, the switching behavior from

oleophobic to superhydrophilic characteristics was observed under the flip-flop motion between the fluoroalkyl groups and the cationic moieties when the environment on the reverse side is changed from oil to water, in addition to the good surface ionic conductivity. In contrast, the surface side affords the usual oleophobic and hydrophobic characteristic imparted by fluoroalkyl groups in the ionogels. Therefore, these fluorinated oligomeric silica ionogels are suggested to have high potential for new fluorinated functional materials through not only the surface active characteristics imparted by longer fluoroalkyl groups but also the excellent properties related to the ionic liquids.

References

1) T. Welton, *Chem. Rev.*, **99**, 2071 (1999).

2) J. Duppont, *Acc. Chem. Res.*, **44**, 1223 (2011).

3) SM. Zakeeruddin and M. Gratzel, *Adv. Funct. Mater.*, **19**, 2187 (2009).

4) L. Bideau, L. Viau, and A. Vioux, *Chem. Soc. Rev.*, **40**, 907 (2011).

5) W. Kubo, T. Kitamura, K. Hanabusa, Y. Wada, and S. Yanagida, *Chem. Commun.*, 374 (2002).

6) J. Lu, F. Yan, and J. Texter, *Prog. Polym. Sci.*, **34**, 431 (2009).

7) T. Fukushima and T. Aida, *Chem. Eur. J.*, **13**, 5048 (2007).

8) P. Wang, SM. Zakeeruddin, P. Comte, I. Exnar, and M. Gratzel, *J. Am. Chem. Soc.*, **125**, 1166 (2003).

9) M-A. Neouze, JL. Bideau, P. Gaveau, S. Bellayer, and A. Vioux, *Chem. Mater.*, **18**, 3931 (2006).

10) SAM. Noor, PM. Bayley, M. Forsyth, and DR. MacFalane, *Electrochimica Acta.*, **91**, 219 (2013).

11) K. Ueno, K. Hata, T. Katakabe, M. Kondoh, and M. Watanabe, *J. Phys. Chem. B.*, **112**, 9013 (2008).

12) K. Ueno, S. Imaizumi, K. Hata, and M. Watanabe, *Langmuir*, **25**, 825 (2009).

13) Y. Yan, T. Jie, J. Xin, and Q. Qi, *J. Appl. Polym. Sci.*, **121**, 1566 (2011).

14) Z. Chen, F. Li, H. Yang, T. Yi, and C. Huang, *Chem. Phys. Chem.*, **8**, 1293 (2007).

15) M. Gorlov and L. Kloo, *Dalton Trans.*, 2655 (2008).

16) K. Matsumoto, T. Fujigaya, H. Yanagi, and N. Nakashima, *Adv. Funct. Mater.*, **21**, 1089 (2011).

17) H. Sawada, *Polym. Chem.*, **3**, 46 (2012).

18) H. Sawada, T. Suzuki, H. Takashima, and K. Takishita, *Colloid Polym. Sci.*, **286**, 1569 (2008).

19) H. Sawada, K. Shima, J. Kyokane, K. Oharu, H. Nakagawa, and T. Kitazume, *Eur. Polym. J.*, **40**, 1595 (2004).

20) H. Sawada and M. Nakayama, *J. Chem. Soc., Chem. Commun.*, 677 (1991).

21) K. Hanabusa, R. Tanaka, M. Suzuki, M. Kimura, and H. Shirai, *Adv. Mater.*, **9**, 1095 (1997).

22) K. Hanabusa, K. Okui, K. Karaki, M. Kimura, and H. Shirai, *J. Colloid Interface Sci.*, **195**, 86 (1997).

23) G. Gallagher, A. Kavanagh, B. Ziolkowski, L. Florea, DR. MacFarlane, K. Fraser, and D. Diamond, *Phys. Chem. Chem. Phys.*, **16**, 3610 (2014).

24) H. Sawada, *Chem. Rev.*, **96**, 1979 (1996).

25) T. Kijima, M. Nishida, H. Fukaya, M. Yoshida, and H. Sawada, *J. Polym. Sci. Part A: Polym. Chem.*, **51**, 2555 (2013).

26) H. Sawada, *Prog. Polym. Sci.*, **32**, 509 (2007).

27) H. Sawada, T. Tashima, Y. Nishiyama, M. Kikuchi, G. Kostov, Y. Goto, and B. Ameduri, *Macromolecules*, **44**, 1114 (2011).

28) M. Mugisawa and H. Sawada, *Langmuir*, **24**, 9215 (2008).

29) H. Sawada and R. Kasai, *Polym. Adv. Technol.*, **16**, 655 (2005).

30) H. Sawada, Y. Okada, Y. Goto, T. Fukui, Y. Shibukawa, S. Kodama, and M. Sugiya, *J.*

Jpn. Soc. Colour Mater., **83**, 368 (2010).

31) X. He, W. Yang, and X. Pei, *Macromolecules*, **41**, 4615 (2008).

32) X. Hu, J. Huang, W. Zhang, M. Li, C. Tao, and G. Li, *Adv. Mater.*, **20**, 4074 (2008).

33) M. Mugisawa, R. Kasai, and H. Sawada, *Langmuir*, **25**, 415 (2009).

CHAPTER 4

Gelation of Ionic Liquids by the Use of Fluoroalkyl End-Capped Oligomers/Polyaniline Composites

4.1. Introduction

There has hitherto been a great deal of attention in polyaniline (PAn), compared with other conducting polymers, due to its relatively simple preparation procedure, good mechanical properties, high environmental stability and its electrical properties which can be easily controlled by simple protonation-deprotonation process.[1 ~ 6)] Ionic liquids are also an equally interesting class of materials, exhibiting a variety of unique properties such as a good thermal stability, non-volatility, good ionic conductivity, and wide electrochemical potential windows.[7 ~ 10)] Ionic liquid gels (ionogels) can be prepared by hybridizing the parent ionic liquids with organic and inorganic component such as organic gelators and silica nanoparticles.[11 ~ 14)] For example, silica-based ionogels can enhance not only the mechanical and transparent properties of the silica gels but also ionic conductivity and thermal stability of the ionic liquids.[15 ~ 17)] From this point of view, it is of particular interest to develop the PAn derivatives imparted by unique properties derived from ionic liquids. In fact, polyanilines have been already prepared by the polymerization of aniline monomers catalyzed by ammonium peroxydisulfate in acidic aqueous media containing ionic liquids[18, 19)], by the oxidation with $KMnO_4$ in the ionic liquid containing a monoprotonic Brønsted acid[20 ~ 23)] and by the electrochemical polymerization of aniline in ionic liquids.[24 ~ 27)] It has

been already reported that the fluoroalkyl end-capped oligomers can form the nanometer size-controlled self-assemblies with the aggregation of the terminal fluoroalkyl segments.[28 ~ 31)] Especially, these fluoroalkyl end-capped oligomeric aggregates can interact with PAn as a guest molecule to afford the corresponding oligomers/PAn nanocomposites through the polymerization of PAn catalyzed by ammonium persulfate in the presence of the corresponding oligomers.[32)] Fluorinated oligomers/PAn nanocomposites thus obtained can exhibit a good dispersibility and stability in water and traditional organic solvents such as methanol imparted by surface active characteristic related to the fluoroalkyl groups in the nanocomposites.[32)] In addition, anatase TiO_2 nanoparticles can be effectively encapsulated into these fluorinated PAn nanocomposite cores to afford the corresponding PAn/TiO_2 nanocomposites possessing the photochromic characteristics relative to the PAn and TiO_2 nanopartices.[33)] Therefore, from the developmental viewpoints of new fluorinated polymeric functional materials imparted by both PAn and ionic liquids, it is deeply desirable to study on the hybridization of fluoroalkyl end-capped oligomers/PAn composites and ionic liquids. Herein, this Chapter shows that hydrophilic fluoroalkyl end-capped 2-methacryloyoxyethenesulfonic acid oligomer [R_F-(CH_2-$CMeCO_2CH_2CH_2SO_3H)_n$-R_F; R_F = $CF(CF_3)OC_3F_7$: R_F-$(MES)_n$-R_F], and fluoroalkyl end-capped 2-acrylamido-2-methylpropanesulfonic acid oligomer [R_F-(CH_2-$CHC(=O)NHCMe_2CH_2SO_3H)_n$-$R_F$; R_F =

$CF(CF_3)OC_3F_7$: R_F-$(AMPS)_n$-R_F] /polyaniline (PAn) nanocomposites can cause the gelation of a variety of hydrophilic ionic liquids, although the parent R_F-$(MES)_n$-R_F and R_F-$(AMPS)_n$-R_F oligomers were not effective for such gelation. This Chapter also shows that the oleophilic fluoroalkyl end-capped *N*-(1,1-dimethyl-3-oxobutyl)acrylamide oligomer [R_F-$(DOBAA)_n$-R_F] can disperse well the original PAn powders into methanol to afford the corresponding oligomer/PAn composites, and the isolated composite powders after the removal of the solvent can cause the gelation for oleophilic ionic liquids. Such gelation behavior of ionic liquids toward the PAn composites is considered to be the first example. These results will be described in this Chapter.

4.2. Experimental

4.2.1. Measurements

Molecular weight of R_F-$(DOBAA)_n$-R_F oligomer (Mn = 4000) was measured using a Shodex DS-4 (pump) and Shodex RI-71 (detector) gel permeation chromatography (Tokyo, Japan) calibrated with polystyrene standard using tetrahydrofuran (THF) as the eluent. Molecular weights of R_F-$(MES)_n$-R_F oligomer (Mn = 13700) and R_F-$(AMPS)_n$-R_F oligomer

(Mn = 20500) were determined by using the same gel permeation chromatography calibrated pullulan (molecular weights: 2000 ~ 50000) and poly(ethylene glycol) (molecular weight: 1000 ~ 40000) standards, respectively, by using 0.5 mol dm^{-3} Na_2HPO_4 aqueous solution as the eluent. Dynamic light scattering (DLS) measurements were measured by using Otsuka Electronics DLS-7000 HL (Tokyo, Japan). Micrometer size-controlled composite particles were measured by using laser diffraction particle size analyzer: Shimadzu SALD-200 V (Kyoto, Japan). Field emission scanning electron micrographs (FE-SEM) were obtained by using JEOL JSM-7000F (Tokyo, Japan). Optical microscopies were measured by using OLYMPUS Corporation BX51 (Tokyo, Japan). Ultraviolet-visible (UV-vis) spectra were recorded by using Shimadzu UV-1600 UV-vis spectrophotometer (Kyoto, Japan).

4.2.2. Materials

Tributylallylphosphonium bis(trifluoromethanesulfonyl)imide [TBAP-BTFSI], triethyl-dodecylphosphonium bis(trifluoromethanesulfonyl)imide [TEDP-BTFSI], triethyldodecyl-ammonium bis(trifluoromethanesulfonyl)imide [TEDA-BTFSI], tributyl-2-hydroxyethyl-phosphonium chloride [TBHEP-Cl] and tributyl[3-(trimethoxysilyl)propyl]phosphonium chloride [TBTMSiP-Cl] were received from Nippon Chemical Industrial Co., Ltd., Tokyo,

Japan. 1-Ethyl-3-methylimidazolium bis(trifluoromethanesulfonyl)imide [EMI-BTFSI] was purchased from Kanto Chemical Co., Ltd., Tokyo, Japan. *N*-Methylpyrazolium tetrafluoroborate [NMP-BF4] was received from Stella Chemifa Corp. (Osaka, Japan). 1-Butyl-3-methylimidazolium hexafluorophosphate [BMI-PF6] was obtained from Merck KGaA (Darmstadt, Germany). 1-Ethyl-3-methylimidazolium hydrogen sulfate [EMI-HSO4] was purchased from Tokyo Chemical Industrial Co., Ltd. (Tokyo, Japan). 2-(Methacrylolyoxy)ethanesulfonic acid and 2-acrylamido-2-methylpropanesulfonic acid were purchased from Polyscience, Inc. (PA, USA) and Wako Pure Chemical Industries, Ltd. (Osaka, Japan), respectively. Aniline was purchased from Tokyo Kasei Kogyo Co., Ltd.. PAn (emeraldine base) was purchased from Sigma-Aldrich Japan (Tokyo, Japan). R_F-$(DOBAA)_n$-R_F oligomer, R_F-$(MES)_n$-R_F oligomer and R_F-$(AMPS)_n$-R_F oligomer were synthesized by reaction of fluoroalkanoyl peroxide with the corresponding monomers according to the previously reported methods.[34 ~ 36)]

4.2.3. Preparation of fluoroalkyl end-capped 2-methacryloyloxyethanesulfonic acid oligomer [R_F-(MES)$_n$-R_F]/PAn nanocomposites

To an aqueous solution (24 ml) of fluoroalkyl end-capped 2-methacryloyloxyethane-sulfonic acid oligomer {R_F-[$CH_2CMeC(=O)OCH_2CH_2SO_3H]_n$-$R_F$ [R_F-(MES)$_n$-R_F]; R_F = $CF(CF_3)OC_3F_7$ (282 mg)}, was added aniline (47 mg). The mixture was stirred with a magnetic stirring bar at room temperature for 30 min. Eleven milliliter of APS (115 mg) aqueous solution was added dropwise to the solution containing aniline and fluorinated oligomer with continuously stirring at room temperature for 1 day. After the removal of solvent, the crude product was purified by the reprecipitaion (H_2O/tetrahydrofuran) to afford the expected R_F-(MES)$_n$-R_F/PAn nanocomposites. The nanocomposites thus obtained were dried in vacuo at 50 ^oC for 2 days to afford green-colored powders (263 mg). R_F-(AMPS)$_n$-R_F/PAn nanocomposites were also prepared under similar conditions to afford dark green-colored powders, respectively.

4.2.4. Dispersion of original PAn powders into methanol by the use of R_F-(DOBAA)$_n$-R_F oligomer

PAn powders (10 mg) was directly added into the transparent homogeneous methanol solution (5.0 ml) containing R_F-(DOBAA)$_n$-R_F oligomer (60 mg). The mixture was stirred well with magnetic stirring bar at room temperature for 2 days to provide the well dispersed blue-green colored fluorinated oligomer/PAn composites.

4.2.5. Gelation of ionic liquids by R_F-(MES)$_n$-R_F/PAn nanocomposites

R_F-(MES)$_n$-R_F/PAn nanocomposites (16 mg), which were prepared under the feed ratios (mg/mg) of the oligomer/aniline: 282/47, was added to 1-ethyl-3-methylimidazolium hydrogen sulfate (250 mg). The resulting mixture was treated under ultrasonic conditions for 3 days at 50 ^oC to afford the R_F-(MES)$_n$-R_F/PAn nanocomposites-based ionogels. Other fluorinated oligomers/PAn compoistes-based ionogels were prepared under similar conditions.

4.2.6. Ionic conductivity measurements

The ionic conductivity of the fluoroalkylated PAn nanocomposites (composites) ionogels was measured by using Agilent Technologies 34401A (Keysight Technologies, Tokyo). The analysis was conducted in the temperature range from 25 to 125 ^{o}C.

4.3. Results and discussion

Fluoroalkyl end-capped 2-methacryloyloxyethanesulfonic acid oligomer [R_F-(MES)$_n$-R_F]/PAn nanocomposites were prepared by the polymerization of aniline monomer initiated by ammonoium persulfate in the presence of the corresponding oligomer according to the previously reported method.[32] Fluoroalkyl end-capped 2-acrylamido-2-methylpropanesulfonic acid oligomer [R_F-(AMPS)$_n$-R_F]/PAn nanocomposites were also prepared under similar conditions. These results are shown in Scheme 4-1 and Table 4-1.

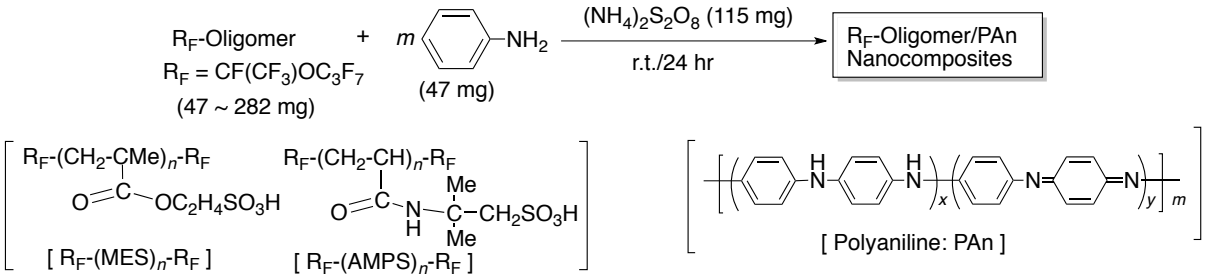

Scheme 4-1 Preparation of R_F-Oligomer/PAn nanocomposites

Table 4-1 Preparation of R_F-Oligomer/PAn nanocomposites

Run	R_F-Oligomer (mg)	Feed ratio of R_F-oligomer/aniline (g/g)	Size of Composites [a] (nm ± STD)
	[R_F-(MES)$_n$-R_F]		
1	47	1.0	98 ± 12
2	94	2.0	103 ± 13
3	188	4.0	33 ± 6
4	282	6.0	33 ± 5
	[R_F-(AMPS)$_n$-R_F]		
5	47	1.0	118 ± 13
6	94	2.0	131 ± 17
7	188	4.0	79 ± 9
8	282	6.0	75 ± 7

a)Cited from Ref. 32

R_F-(MES)$_n$-R_F/PAn nanocomposites (Run 4 in Table 4-1) interacted with 1-ethyl-3-methylimidazolium hydrogen sulfate to cause the gelation as shown in Fig. 4-1.

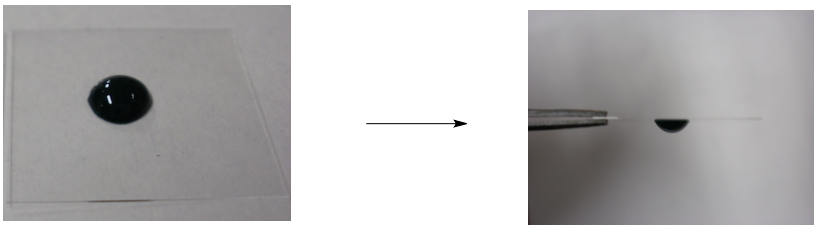

Fig. 4-1 Photograph of R_F-$(MES)_n$-R_F/PAn nanocomposite ionogel (ionic liquid: EMI-HSO4)

EMI-HSO_4:  $HSO_4^{\ominus}$

The gelling ability for other R_F-$(MES)_n$-R_F/PAn nanocomposites (Runs 1 ~ 3) in Table 4-1 was studied under the similar conditions, and each composite can form the gel toward EMI-HSO4. To study the gel-formation ability, the minimum concentrations of the R_F-$(MES)_n$-R_F/PAn nanocomposites necessary for gelation have been measured according to a method reported by Hanabusa et al.[37, 38], and the results on the minimum concentration for gelation (C_{min}) in EMI-HSO4 at 25 °C are shown in Table 4-2.

Table 4-2 The minimum gel concentrations (C_{mim}) of R_F-$(MES)_n$-R_F/PAn nanoconposites

	C_{mim}
Run 1*	13
Run 2*	10
Run 3*	6
Run 4*	6

* Each Run No corresponds to that of Scheme 4-1

C_{min}s of the R_F-$(MES)_n$-R_F/PAn nanocomposites necessary to gel of EMI-HSO4 are 6 ~

13 wt%. The R_F-$(MES)_n$-R_F/PAn nanocomposites, which were prepared under the higher feed ratios (188 ~ 282 mg) of the oligomer toward aniline monomer (47 mg), were found to decrease the C_{min} values from 13 to 6 wt % to provide a higher gelling ability, indicating that sulfo segments in the oligomer should interact effectively with the basic moieties in the PA in the composites to produce the additional ionic network cores. Such ionic network cores are likely to interact with the ionic liquid to form the ionogels.

The gelling ability of a variety of ionic liquids illustrated in Fig. 4-2 was studied by the use of R_F-$(MES)_n$-R_F/PAn nanocomposites (Run 4 in Table 4-1) and R_F-$(AMPS)_n$-R_F/PAn nanocomposites (Run 8 in Table 4-1). The results are shown in Table 4-3.

Structure	Abbreviation	Structure	Abbreviation
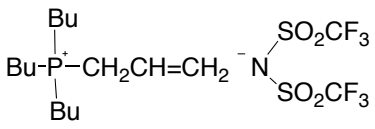	[TBAP-BTFSI]	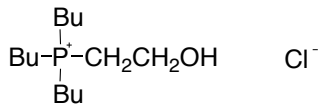	[TBHEP-Cl]
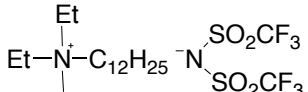	[TEDA-BTFSI]	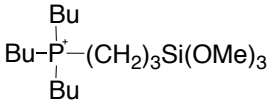	[TBTMSiP-Cl]
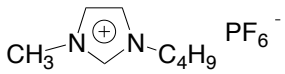	[BMI-PF6]	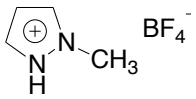	[NMP-BF4]
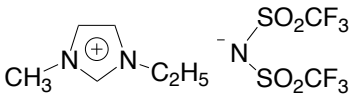	[EMI-BTFSI]	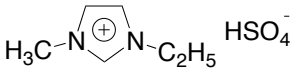	[EMI-HSO4]
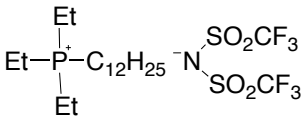	[TEDP-BTFSI]		

Fig. 4-2 Molecular structures and abbreviations of ionic liquids used

Table 4-3 Dispersibility and C_{min} of R_F-(MES)$_n$-R_F/PAn and R_F-(AMPS)$_n$-R_F/PAn nanocomposites toward a variety of ionic liquids

Ionic Liquid	R_F-(MES)$_n$-R_F/PAn nanocomposites C_{min} (%)	R_F-(AMPS)$_n$-R_F/PAn nanocomposites C_{min} (%)
TBAP-BTFSI	---*	---*
TEDA-BTFSI	---*	---*
BMI-PF6	---*	---*
EMI-BTFSI	---*	---*
TEDP-BTFSI	---*	---*
TBHEP-Cl	13	6
TBTMSiP-Cl	2	2
NMP-BF4	7	4
EMI-HSO4	6	4

*not dispersible

Original R_F-(MES)$_n$-R_F oligomer and R_F-(AMPS)$_n$-R_F oligomer were not effective for the gelation of the ionic liquids illustrated in Fig. 4-2. However, as shown in Table 4-3, the R_F-(MES)$_n$-R_F/PAn nanocomposites and the R_F-(AMPS)$_n$-R_F/PAn nanocomposites were found to cause the gelation toward the hydrophilic ionic liquids such as TBHEP-Cl, TBTMSiP-Cl, NMP-BF4, and EMI-HSO4. On the othe hand, these nanocomposites cannot provide a dispersibility at all toward the oleophilic ionic liquids such as TBAP-BFSI, TEDA-BTFSI, BMI-PF6, EMI-BTFSI, and TEDP-BTFSI. This finding is due to the hydrophilic characteristic of the R_F-(MES)$_n$-R_F/PAn nanocomposites and the R_F-(AMPS)$_n$-R_F/PAn nanocomposites.

In this way, it was clarified that these hydrophilic R_F-$(MES)_n$-R_F/PAn nanocomposites and R_F-$(AMPS)_n$-R_F/PAn nanocomposites can interact with the hydrophilic ionic liquids to provide the ionogels. To verify the ionogel formation derived from the fluorinated PAn nanocomposites, the FE-SEM measurements of the R_F-$(AMPS)_n$-R_F/PAn nanocomposite ionogels (ionic liquid: TBTMSiP-Cl) have been studied, and the results are shown in Fig. 4-3.

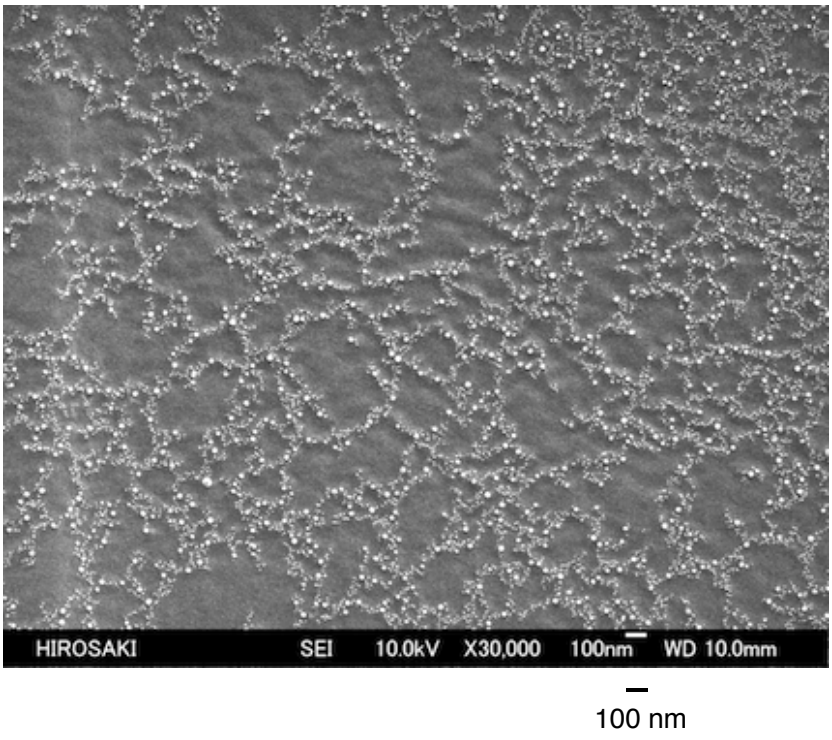

Fig. 4-3 Field emission scanning electron microscopy [FE-SEM] Images of R_F-$(AMPS)_n$-R_F/PAn nanocomposite ionogel (ionic liquid: TBTMSiP-Cl)

As shown in Fig. 4-3, the clear network structures can be observed in the FE-SEM images of the R_F-$(AMPS)_n$-R_F/PAn nanocomposite ionogels. Similar network structures have been also observed in the *N*-isopropylacrylamide polymer ionogels.[39)]

The R_F-$(MES)_n$-R_F/PAn nanocomposite ionogels for their ionic conductivities have been tested at various temperatures between 25 and 125 °C. The results are shown in Figs. 4-4 and 4-5, together with that of the parent ionic liquid, for comparison.

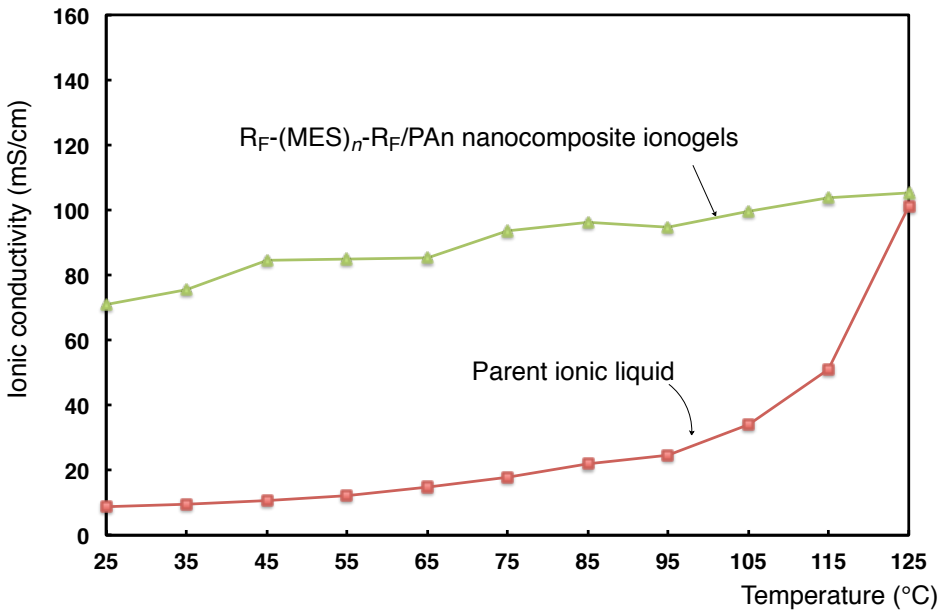

Fig. 4-4 Temperature dependencies of the ionic conductivities of R_F-$(MES)_n$-R_F/PAn nanocomposite ionogels (ionic liquid: EMI-HSO4) and the original EMI-HSO4: Concentration of gelator; 10 wt %

As shown in Fig. 4-4, the ionic conductivities of the fluorinated PAn nanocomposite ionogels were found to increase with the increase of temperatures, and a higher conductivity than that of the original ionic liquids was obtained from 25 to 115 °C. More interestingly, the ionic conductivities at 125 °C can keep the similar values even after 10 hrs, as well as those of the original ionic liquids (see Fig. 4-5). Therefore, these fluorinated PAn nanocomposite ionogels are promising candidates for the fuel cells.

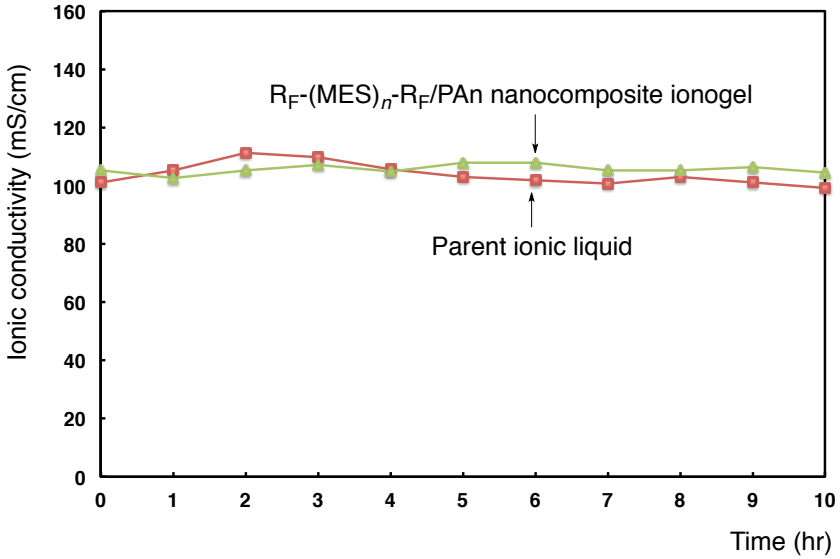

Fig. 4-5 Time dependencies of the ionic conductivities of R_F-$(MES)_n$-R_F/PAn nanocomposite ionogels (ionic liquid: EMI-HSO4) and the original EMI-HSO4 at 125 ºC: Concentration of gelator: 10 wt %

Hitherto, it is well known that fluoroalkyl end-capped oligomers are attractive functional materials, because they exhibit numerous unique properties such as high solubility, surface active properties, biological activities, and nanometer size-controlled self-assembled molecular aggregates through the aggregation of terminal fluoroalkyl groups which cannot be achieved by the corresponding non-fluorinated and randomly fluoroalkylated ones.[30, 31] The fluorinated oligomeric aggregates can interact with a variety of guest molecules such as fullerene, carbon nanotube, silica nanoparticles and titanium oxide nanoparticles to afford the corresponding fluorinated oligomers/guest molecules nanocomposites.[30, 40, 41] As mentioned above, these fluorinated oligomers/PAn nanocomposites can exhibit a hydrophilic characteristic to form the hydrophilic ionogels through the interaction with the hydrophilic ionic liquids. From the developmental viewpoint of new hydrophobic PAn composite

ionogels, it is of particular interest to study on the dispersion of the original PAn powders into the organic medium by the use of the hydrophobic fluoroalkyl end-capped oligomers such as fluoroalkyl end-capped *N*-(1,1-dimethyl-3-oxobutyl)acrylamide oligomer [R_F-(DOBAA)$_n$-R_F; R_F = $CF(CF_3)OC_3F_7$]. In fact, the original PAn powders into the R_F-(DOBAA)$_n$-R_F oligomer methanol solution are tried to disperse by stirring the mixture with magnetic stirring bar at room temperature for 2 days. The original PAn powders have been also tried to disperse into the non-fluorinated DOBAA oligomer methanol solution, for comparison. These results are shown in Scheme 4-2 and Table. 4-4.

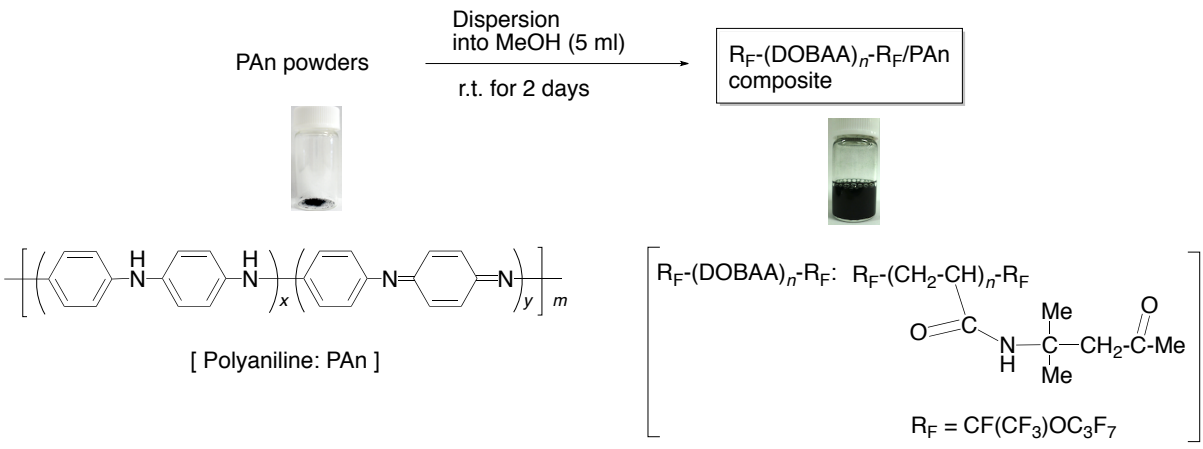

Scheme 4-2 Dispersion of the original PAn powders into methanol by the use of R_F-(DOBAA)$_n$-R_F oligomer

Table 4-4 Dispersion of the original PAn powders into methanol by the use of R_F-(DOBAA)$_n$-R_F oligomer

	PAn powders (mg)	R_F-(DOBAA)$_n$-R_F (mg)	Size of the composites (μm)*
Run 1	10	20	16.7 ± 0.2
Run 2	10	60	11.6 ± 0.2
		-(DOBAA)$_n$-	
Run 3	10	60	160.6 ± 0.1
Original PAn			188.9 ± 0.1

*) Determined by laser diffraction particle size analyzer

As shown in Scheme 4-2 and Table 4-4, the well-dispersed PAn blue-green colored methanol solution were prepared by using R_F-(DOBAA)$_n$-R_F oligomer, and the sizes of the well-dispersed R_F-(DOBAA)$_n$-R_F/PAn composites are micrometer-size controlled from 12 to 17 μm. The higher size (189 μm) of the parent PAn than that of the obtained composites is due to the agglomeration or the aggregation of the original PAn powders in methanol.

UV-vis spectra of well-dispersed R_F-(DOBAA)$_n$-R_F/PAn composite methanol solutions [Fig. 4-6-(b) and (c)] can exhibit the two absorption peaks around at 325 and 640 nm, which are due to the π-π* transition of the benzenoid rings and the excitation absorption of the quinoid rings, respectively (see Fig. 4-6).[42)]

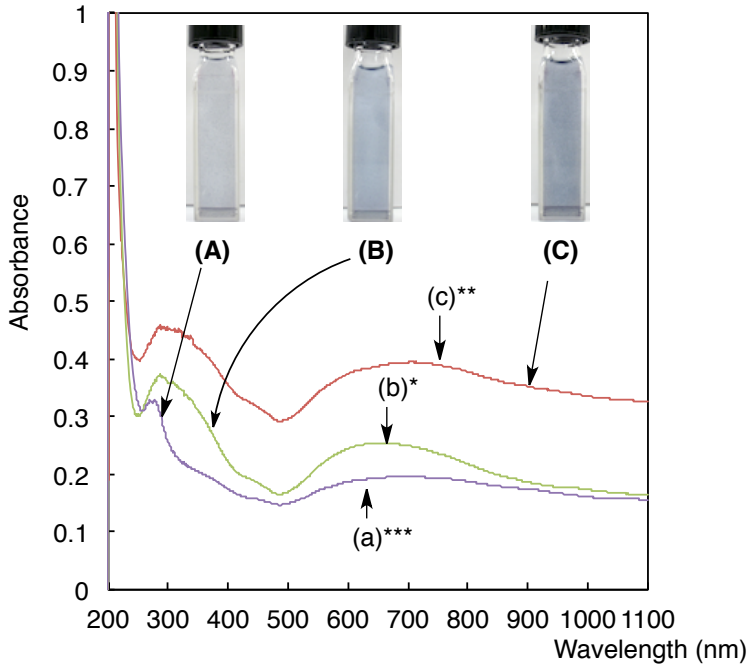

FIg. 4-6 UV-vis spectra of R_F-(DOBAA)$_n$-R_F/PAn composites (**b, c**) and –(DOBAA)$_n$–/PAn composites (**a**) in methanol and photograph of these methanol solutions (**A** ~ **C**)

*) Concentration of oligomer (Run 1 in Scheme 2: 86 mg/dm^3); concentration of PAn (43 mg/dm^3)

**) Concentration of oligomer (Run 2 in Scheme 2: 258 mg/dm^3); concentration of PAn (43 mg/dm^3)

***) Concentration of oligomer (Run 3 in Scheme 2: 258 mg/dm^3); concentration of PAn (43 mg/dm^3)

Such higher absorption peaks can afford the deeper blue-green colored solutions [see Fig. 4-6-(B) and (C)]. On the other hand, the non-fluorinated DOBAA oligomer [Fig. 4-6-(a) and (A)] was not effective for enhancing the absorption peaks around at 325 and 640 nm related to the PAn, indicating that the non-fluorinated DOBAA oligomer cannot form the molecular aggregates to interact with the PAn as a guest molecule, quite different from that of the R_F-(DOBAA)$_n$-R_F oligomer. Because, it is well known that R_F-(DOBAA)$_n$-R_F oligomer can form the nanometer size-controlled self–assemblies with the aggregation of terminal fluoroalkyl segments to interact with a variety of guest molecules such as fullerene and

carbon nanotube.[39 ~ 41)]

Next, the gelling ability of the oleophilic ionic liquids such as EMI-BTFSI and TBHEP-Cl by using R_F-(DOBAA)$_n$-R_F/PAn composites were studied under the similar conditions to that of R_F-(MES)$_n$-R_F/PAn nanocomposites. Interestingly, the R_F-(DOBAA)$_n$-R_F/PAn composites were found to be effective for the gelation of the ionic liquids (see Fig. 4-7). The C_{min} values at 25 °C are shown in Table 4-5.

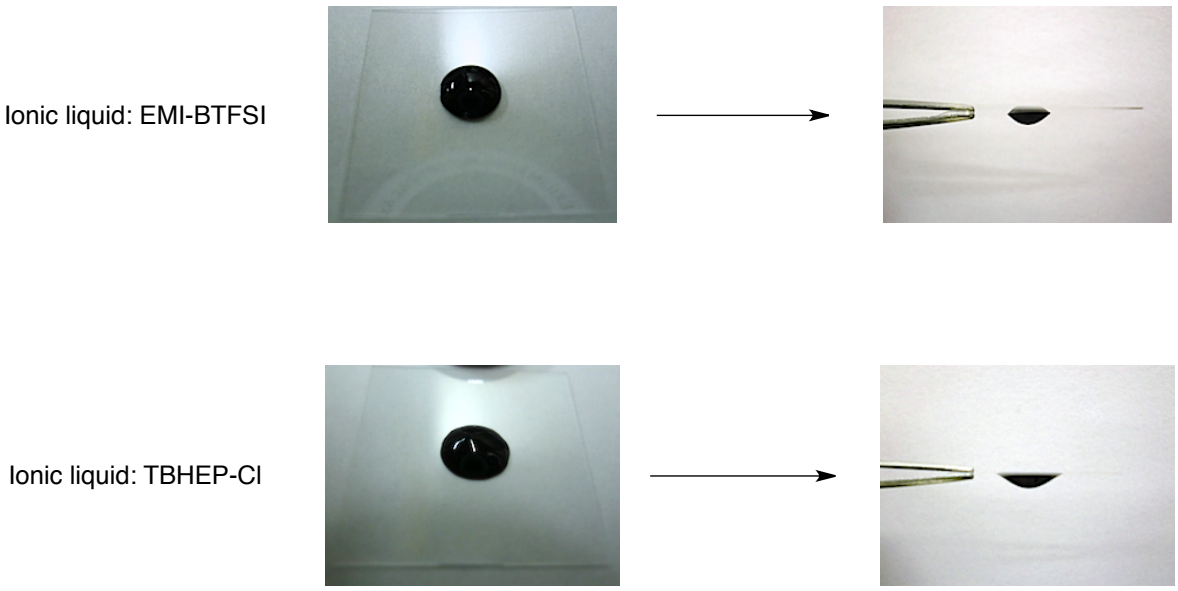

Fig. 4-7 Photograph of R_F-(DOBAA)$_n$-R_F/PAn composite ionogels (ionic liquids: EMI-BTFSI, TBHEP-Cl)

EMI-BTFSI: 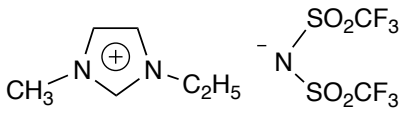

TBHEP-Cl: 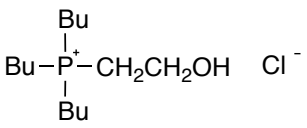

Table 4-5 The C_{min} values at 25 ℃ of the R_F-(DOBAA)$_n$-R_F/PAn composite ionogels

Ionic liquid	C_{min}
EMI-BTFSI	18
TBHEP-Cl	20

In this case, since TBHEP-Cl can exhibit an amphiphilic characteristic, TBHEP-Cl should be selected as a suitable ionic liquid for both the hydrophilic and oleophilic gelators. In contrast, the R_F-(DOBAA)$_n$-R_F/PAn composites have been shown to exhibit no gelling ability toward hydrophilic ionic liquids such as EMI-HSO4. This finding is due to the oleophilic characteristic of this composite.

In order to clarify the formation of the R_F-(DOBAA)$_n$-R_F/PAn composite ionogels, the optical microscopy of the R_F-(DOBAA)$_n$-R_F/PAn composite methanol solution has been studied. In addition, the FE-SEM measurements of the R_F-(DOBAA)$_n$-R_F/PAn composite ionogel have been also studied. These results are shown in Figs. 4-8 and 4-9.

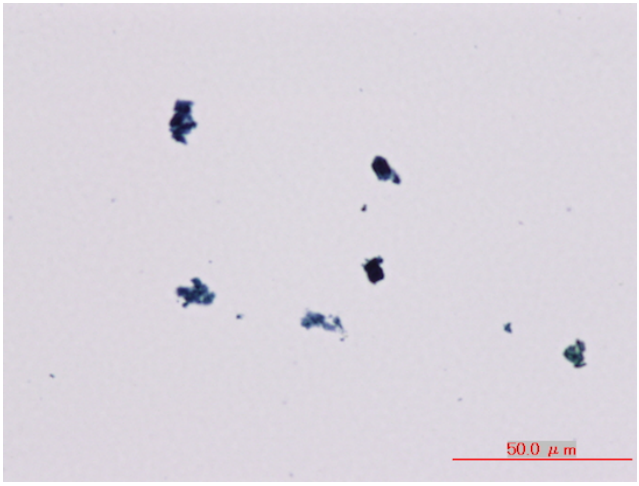

Fig. 4-8 Optical microscopic image of the R_F-(DOBAA)$_n$-R_F/PAn composite (Run 2 in Scheme 4-2, Table 4-4) methanol solution

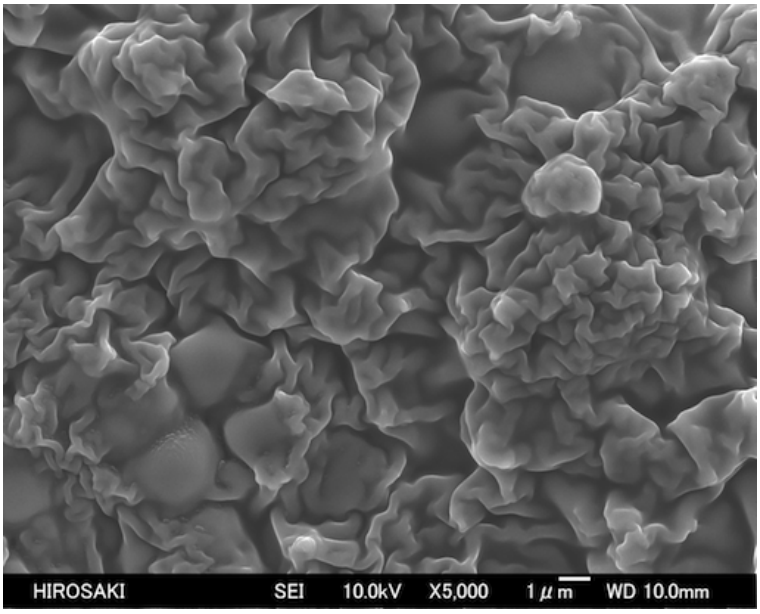

Fig. 4-9 FE-SEM image of the R_F-(DOBAA)$_n$-R_F/PAn ionogel (ionic liquid: EMI-BTFSI) Concentration of gelator: 30 wt %

As shown in Fig. 4-8, it was demonstrated that the PAn can be effectively encapsulated into the R_F-(DOBAA)$_n$-R_F oligomeric aggregate cores to provide the corresponding

fluorinated oligomer/PAn composite. The size (~ 10 μm) of the composite determined by the optical microscopy is the same to that (12 μm) by laser diffraction particle size analyzer illustrated in Table 4-4. The FE-SEM picture of the R_F-(DOBAA)$_n$-R_F/PAn composite ionogel (see Fig. 4-9) is quite different from that of the R_F-(MES)$_n$-R_F/PAn nanocomposite ionogel which consists of the clear network structures illustrated in Fig. 4-3. This suggest that the composite ionogel would be built up through the electrostatic interaction between the R_F-(DOBAA)$_n$-R_F/PAn composite aggregates and the ionic liquid.

The ionic conductivity (27 mS/cm) of the R_F-(DOBAA)$_n$-R_F/PAn composite ionogels (ionic liquids: TBHEP-Cl) was found to increase slightly, compared with that (21 mS/cm) of the parent ionic liquid. On the other hand, the R_F-(MES)$_n$-R_F/PAn nanocomposite ionogels can increase the ionic conductivity more efficiently than that of the parent ionic liquid as shown in Fig. 4-4. This finding is due to the structural difference of the PAn between the R_F-(DOBAA)$_n$-R_F/PAn composites and the R_F-(MES)$_n$-R_F/PAn nanocomposites. Because, the R_F-(MES)$_n$-R_F oligomer possesses the higher acidic moieties such as sulfo groups to interact with the emeraldine base units in the PAn in the nanocomposites to produce the partially protonated PAn units (the doped state: the emelaridine salts) as in Fig. 4-10.

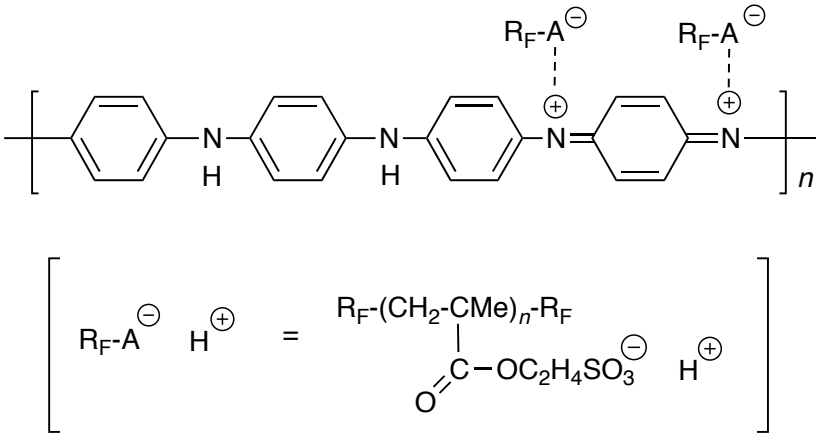

Fig. 4-10 Schematic illustration for the partially protonated PAn in the nanocomposites

Such protonated PAn units should enhance the ionic conductivities of the corresponding ionogels.

The higher C_{min} values (18 ~ 20 wt%) of the R_F-$(DOBAA)_n$-R_F/PAn composite ionogels than those (2 ~ 13 wt%) of the R_F-$(MES)_n$-R_F/ and R_F-$(AMPS)_n$-R_F/PAn nanocomposite ionogels indicate that the gelling ability of these ionogels is inferior to that of the nanocomposite ionogels. This finding suggests that the R_F-$(MES)_n$-R_F/ and R_F-$(AMPS)_n$-R_F/PAn nanocomposite ionogels should be built up through the synergistic interaction of both the aggregation of the end-capped fluoroalkyl segments and the ionic interaction between the ionic liquids and the emelaridine salts in the nanocomposites as in Fig. 4-10. In contrast, the R_F-$(DOBAA)_n$-R_F/PAn composites, which were prepared by the encapsulation of the PAn into the fluorinated oligomeric aggregate cores, should interact with

the ionic liquid through the electrostatic interaction with the basic moieties in the PAn to produce the ionogels. The gelling ability of such ionogels which were built up through the electrostatic interaction would be inferior to that of the corresponding fluorinated oligomers/PAn nanocomposite ionogels.

4.4 Conclusions

Hydrophilic fluoroalkyl end-capped oligomers such as R_F-$(MES)_n$-R_F oligomer and R_F-$(AMPS)_n$-R_F oligomer were applied to the preparation of R_F-$(MES)_n$-R_F/ and R_F-$(AMPS)_n$-R_F/PAn nanocomposites. These fluorinated oligomers/PAn nanocomposites can interact with the hydrophilic ionic liquids to produce the corresponding fluorinated oligomers/PAn nanocomposite ionogels. However, these fluorinated oligomers/PAn nanocomposites cannot interact with the oleophilic ionic liquids to produce the corresponding nanocomposite ionogels. Oleophilic R_F-$(DOBAA)_n$-R_F oligomer was applied to the dispersion of the original PAn powders into methanol. The obtained R_F-$(DOBAA)_n$-R_F/PAn composites after the removal of the solvent were found to cause the gelation for not hydrophilic but oleophilic ionic liquids including the amphiphilic ionic liquid. The ionic conductivities of the R_F-$(MES)_n$-R_F/PAn nanocomposite ionogels were found to increase

effectively, compared with that of the original ionic liquid. On the other hand, the R_F-$(DOBAA)_n$-R_F/PAn composite ionogel was not so effective for the increase of the ionic conductivity. The higher ionic conductivity of the R_F-$(MES)_n$-R_F/PAn nanocomposite ionogels is due to the presence of the acid-doped emelaridine salts in the PAn units. In this way, it was verified that the present fluorinated oligomers/PAn nanocomposites (composites) have high potential for novel gelators toward not only the hydrophilic but also oleophilic ionic liquids including the amphiphilic ionic liquids.

References

1) S. Bhadra, D. Khastgir, N. K. Singha, and J. H. Lee, *Prog. Polym. Sci*., **34**, 783 (2009).

2) J. Stejskal, I. Sapurina, and M. Trchova, *Prog. Polym. Sci*., **35**, 1420 (2010).

3) M. Wan, *Macromol. Rapid Commun*., **30**, 963 (2009).

4) J. Huang, S. Virji, B. H. Weller, and R. B. Kaner, *Chem. Eur. J*., **10**, 1314 (2004).

5) N. D. Debarnot and P. F. Epaillard, *Anal. Chimica. Acta*., **475**, 1 (2001).

6) E. T. Kang, K. G. Neoh, and K. L. Tan, *Prog. Polym. Sci*., **23**, 277 (1998).

7) C. A. Angell, Y. Ansari, and Z. Zhao, *Faraday Discuss*., **154**, 9 (2012).

8) D. S. Silvester, *Analyst*, **136**, 4871 (2011).

9) J. Lu, F. Yan, and J. Texter, *Prog. Polym. Sci*., **34**, 431 (2009).

10) T. Torimoto, T. Tsida, K. Okazaki, and S. Kuwabata, *Adv. Mater*., **22**, 1196 (2010).

11) J. L. Bideau, L. Viau, and A. Vioux, *Chem. Soc. Rev*., **40**, 907 (2011).

12) H. Hu, W. Yuan, H. Zhao, and G. L. Baker, *J. Polym. Sci., Paert A: Polym. Chem*., **52**, 121 (2014).

13) Z. Ma, J. Yu, and S. Dai, *Adv. Mater*., **22**, 261 (2010).

14) Z. –L. Xie, X. Huang, and A. Taubert, *Adv. Funct. Mater*., **24**, 2837 (2014).

15) P. Wang, S. M. Zakeeruddin, P. Comte, I. Exnar, and M. Gratzel, *J. Am. Chem. Soc*., **125**, 1166 (2003).

16) J. A. Marins, Soares, A. A. Siva, M. G. Hurtado, and S. Livi, *J. Colloid Interface Sci*., **405**, 64 (2013).

17) S. A. M. Noor, P. M. Bayley, M. Forsyth, and D. R. MacFarlane, *Electrochimica Acta*, **91**, 219 (2013).

18) D. Pahovnik, E. Zagar, K. Kogej, J. Vohlidal, and M. Zigon, *Eur. Polym. J*., **49**, 1381 (2013).

19) N. Bicak, B. F. Senkal, and E. Sezer, *Synthtic Metals*, **155**, 105 (2005).

20) E. Margaretta, C. Olmeda, and L. Yu, *J. Apply. Polym. Sci*., **127**, 2453 (2013).

21) G. A. Snook, T. L. Greaves, and A. S. Best, *J. Mater. Chem*., **21**, 7622 (2011).

22) Y. Ai, F. Zhao, and B. Zeng, *Anal. Methods*, **6**, 9453 (2014).

23) F. F. C. Bazito, L. T. Siveira, R. M. Torresi, and S. I. C. de Torresi, *Phys. Chem. Chem. Phys*., **10**, 1457 (2008).

24) Y. Ai, F. Zhao, and B. Zeng, *Anal. Chim. Acta*, **880**, 60 (2015).

25) B. –Y. Liu, D. -Q. Xu, and Z. –Y. Xu, *Chinese J. Chem*., **23**, 803 (2005).

26) K. Sekiguchi, M. Atobe, and T. Fuchigami, *J. Electroanal. Chem*., **557**, 1 (2003).

27) X.-H. Li, L. Dai, Y. Liu, X.-J. Chen, W. Yan, L.-P. Jiang, and J.-J. Zhu, *Adv. Funct. Mater*., **29**, 3120 (2009).

28) H. Sawada, *Chem. Rev*., **96**, 1979 (1996).

29) H. Sawada, *J. Fluorine Chem*., **121**, 111 (2003).

30) H. Sawada, *Polym. Chem*., **3**, 46 (2012).

31) H. Sawada, *Prog. Polym. Sci.*, **32**, 509 (2007).

32) H. Sawada, T. Tsuzuki-ishi, T. Kijima, M. Iizuka, and M. Yoshida, *Colloid Polym. Sci*., **289**, 1103 (2011).

33) H. Sawada, T. Tsuzuki-ishi, T. Kijima, J. Kawakami, M. Iizuka, and M. Yoshida, *J. Colloid Interface Sci*., **359**, 461 (2011).

34) H. Sawada, Y. Yoshino, M. Kurachi, T. Kawase, K. Takishita, and T. Tanedani, *Polymer*, **41**, 397 (2000).

35) H. Sawada, A. Ohashi, M. Baba, T. Kawase, and Y. Hayakawa, *J. Fluorine Chem*., **79**, 149 (1996).

36) H. Sawada, S. Katayama, Y. Ariyoshi, T. Kawase, Y. Hayakawa, T. Yomota, and M. Baba, *J. Mater. Chem*., **8**, 1517 (1998).

37) K. Hanabusa, R. Tanaka, M. Suzuki, M. Kimura, and H. Shirai, *Adv. Mater*., **9**, 1095 (1997).

38) K. Hanabusa, K. Okui, K. Karaki, M. Kimura, and H. Shirai, *J. Colloid Interface Sci*., **195**, 86 (1997).

39) S. Gallagher, A. Kavanagh, B. Ziolkowski, L. Florea, D. R. MacFarlane, K. Fraser, and D. Diamond, *Phys. Chem. Chem. Phys*., **16**, 3610 (2014).

40) H. Sawada, J. Iidzuka, T. Maekawa, R. Takahashi, T. Kawase, K. Oharu, H. Nakagawa, and K. Ohira, *J. Colloid Interface Sci*., **263**, 1 (2003).

41) H. Sawada, J. Iidzuka, T. Kawase, K. Oharu, and H. Nakagawa, *Eur. Polym. J*., **39**, 1991 (2003).

42) S. –A. Chen and H. –T. Lee, *Macromolecules*, **28**, 2858 (1995).

Conclusions

The results obtained from this study are summarized as follows:

1. Cross-linked fluoroalkyl end-capped acrylic acid cooligomer containing poly(oxyethylene) units can form the nanometer size-controlled fine particles in aqueous solutions, and these cross-linked nanoparticles interact with cytochrome *c* (Cyto-*c*) to afford the corresponding cooligomeric nanoparticles-encapsulated Cyto-*c*, effectively. Interestingly, the fluorinated nanoparticles-encapsulated Cyto-*c* poweder are easily isolated by the simple centrifugal separation of the corresponding aqueous solutions. The cross-linked fluorinated cooligomer also enables an effective transfer of Cyto-*c* from aqueous solution to ionic liquids such as 1-ethyl-3-methylimidazolium bis(trifluoromethanesulfonyl)imide to afford the immobilized Cyto-*c* with the corresponding fluorinated cooligomer in quantitatively immobilized ratio (~ 100 %). The immobilized Cyto-*c* exhibited a good dispersibility in the parent ionic liquid to afford the nanometer size-controlled fluorinated particles-encapsulated Cyto-*c*. Similarly, the cross-linked fluorinated cooligomer in ionic liquids such as 3-methylpyrazolium tetrafluoroborate (3MP-BF4) interacted with Cyto-*c* to afford the corresponding nanoparticles-encapsulated Cyto-*c* in quantitatively encapsulated ratio

(~100 %). These cross-linked fluorinated nanoparticles-encapsulated Cyto-*c* in water and ionic liquids were applied to the oxidation of guaiacol with hydrogen peroxide, and an extremely higher catalytic activity for this oxidation was observed in the ionic liquid (3MP-BF4).

2. New fluoroalkyl end-capped vinyltrimethoxysilane oligomer - ionic liquid silica nanocomposites were prepared by sol-gel reaction of the corresponding oligomer in the presence of phosphorus-type ionic liquid: tri-*n*-butyl[3-(trimethoxysilyl)-propyl]-phosphonium chloride under alkaline conditions. These fluorinated nanocomposites were found to apply to the surface modification of glass, and the modified glass surface exhibited a high oleophobicity imparted by fluoroalkyl groups in nanocomposites. Interestingly, this modified glass surface was found to show superhydrophilicity derived from hydrophilic cationic ionic liquid segments through the flip-flop motion between fluoroalkyl groups and the ionic liquid segments in nancomposites when the surface environment is changed from air to water.

3. Fluoroalkyl end-capped vinyltrimethoxysilane oligomer [R_F-(CH_2-$CHSi(OMe)_3$)$_n$-R_F; n = 2, 3; R_F = $CF(CF_3)OC_3F_7$: R_F-(VM)$_n$-R_F] can undergo the sol-gel reaction under alkaline

conditions at room temperature to provide the corresponding fluorinated oligomeric silica nanoparticles [R_F-(VM-SiO_2)$_n$-R_F]. Silica nanoparticles and tetraethoxysilane are used to the similar sol-gel reaction to prepare the fluoroalkyl end-capped oligomeric silica nanoparticles [R_F-(VM-SiO_2)$_n$-R_F/SiO_2]. These obtained two-type fluorinated oligomeric silica nanoparticles cannot afford the gel toward water and traditional organic media such as methanol and ethanol; however, interestingly these fluorinated nanoparticles can cause a gelation in a variety of ionic liquids such as phosphonium, ammonium, pyrazolium and imidazolium salts-type ionic liquids. These fluorinated oligomeric silica nanoparticles/ionic liquid gels (ionogels) were found to provide a similar ionic conductivity to that of the corresponding parent ionic liquids under a variety of temperatures from 25 to 125 ^oC, and these fluorinated ionogels can keep the similar ionic conductivity even after 10 hrs at 125 ^oC. In addition, these fluorinated oligomeric silica/ionogels are applied to the surface modification of PMMA to exhibit not only surface active characteristic imparted by longer fluoroalkyl groups but also a good ionic conductivity related to the ionic liquid on the surface. More interestingly, the modified PMMA film can afford the switching behavior from oleophobic to superhydrophilic characteristics derived from the flip-flop motion between the fluoroalkyl groups and the cationic moieties when the environment on the reverse side is changed from oil to water.

4. Hydrophilic R_F-$(MES)_n$-R_F/ and R_F-$(AMPS)_n$-R_F/polyaniline (PAn) nanocomposites were prepared by the polymerization of aniline monomer in the presence of the corresponding oligomers. These fluorinated PAn nanocomposites were able to cause the gelation toward a variety of hydrophilic ionic liquids, although the parent R_F-$(MES)_n$-R_F and R_F-$(AMPS)_n$-R_F oligomers were not effective for the gelation of such ionic liquids. Oleophilic R_F-$(DOBAA)_n$-R_F oligomer has no gelling ability toward the ionic liquids; however, this oligomer was able to disperse well the original PAn powders into methanol to afford the corresponding oligomer/PAn composites. Interestingly, the isolated composite powders after the removal of the solvent were found to cause the gelation toward some oleophilic ionic liquids. In these composites, R_F-$(MES)_n$-R_F/PAn nanocomposite/ionic liquid gel (ionogel) was found to provide a higher ionic conductivity than that of the parent ionic liquid under the similar conditions.

Publications

1) Y. Okada (Sutoh) and H. Sawada, "Preparation of novel cross-linked fluoroalkyl end-capped cooligomeric nanoparticles-encapusulated cytochrome *c* in water and ionic liquids", *Colloid Polym. Sci.*, **287**, 1359 (2009).

2) H. Sawada, Y. Okada (Sutoh), Y. Goto, T. Fukui, T. Shibukawa, S. Kodama, and M. Sugiya, "Application of ionic liquid as surface modifier: Switching behavior of novel fluoroalkyl end-capped vinyltrimethoxysilane oligomer – Tri-*n*-butyl-[(3-trimethoxysilyl)propyl] phosphonium chloride silica nanocomposites between superhydrophilicity and oleophobicity", *J. Jpn. Colour Mater.*, **83**, 368 (2010).

3) Y. Sutoh, T. Tsuzuki-ishi, M. Sugiya, and H. Sawada, "Preparation and applications of fluoroalkyl end-capped vinyltrimethoxysilane oligomeric nanoparticle ionogels", *J. Sol-Gel. Sci. Technol.,* **79**, 210 (2016).

4) Y. Sutoh, T. Tsuzuki-ishi, M. Sugiya, and H. Sawada, “Gelation of ionic liquids by the use of fluoroalkyl end-capped oligomers/polyaniline composites”, *Polymer. Composites*, DOI 10.1002/pc.23921, pp 1 – 8 (2016).

Acknowledgements

The author sincerely thanks Prof. Hideo Sawada for his enormous support and insightful comments during the course of his study. Without Prof. Hideo Sawada's guidance and persistent help, this thesis would not have materialized.

Special thanks go to Prof. Isoshi Nukatsuka, Prof. Masaaki Okazaki, Associate Prof. Ryo Miyamoto, and Associate Prof. Masaki Hagihara, who provided valuable comments and discussions to this study, respectively. The author would like to thank to Dr. Taiki Tsuzuki-ishi, past member of Sawada Laboretory for kind advice and discussions. He would also like to thank present and past members of Sawada Laboratory for their generous cooperation and encouragements in everyday life.

Finally, the author would like to express his gratitude to his family and friends and his colleagues in his company who gave moral support and warm encouragements.